Contents

1 Treatment planning for experimental irradiation of cardiac target volumes in porcine data

Contents

An experimental validation of the here presented non-invasive treatment modality for cardiac target sites will be carried out at GSI in 2014. These experiments will be carried out in collaboration with HIT and Uniklinik Heidelberg as well as the Mayo Clinic (Minnesota, USA). Animal models will be used and the study results will be compared to findings with photon irradiation [Sha10] [Bla13]. For the feasibility study different cardiac target sites are possible: PV isolation, ablation of the CTI as well as the AV node. In a first iteration of the experiments, only the AV node of the pigs will be irradiated, both at Mayo Clinic with photons and at GSI with carbon ions. The experiments are planned to enable a direct comparison between particle therapy and photon irradiation, hence many of the treatment settings are kept constant inbetween the two centers. Also in pigs, the cardiac target sites move due to respiration as well as heartbeat. As

the breathing motion of the pigs will be compensated with a respirator, only the influence of heartbeat motion will be studied in more detail. Rescanning as motion mitigation technique will be presented.

1.1 Material and methods

Details on the used input data as well as the used treatment planning parameters will be given. Afterwards an overview over all studies will be given. Finally, the analysis proceeding will be described.

1.1.1 Treatment planning input data

For treatment planning studies with the in-house treatment planning software TRiP4D [Ric13], 4DCT data sets, target and OAR contours as well as a deformable image registration for motion assessment in-between the different motion phases are needed.

In order to assess the motion of the potential cardiac target sites (PV, CTI and AV node) in pigs under influence of heartbeat motion ECG gated 4DCTs were studied. Four porcine data sets were recorded at Mayo Clinic (Minnesota, USA). Thereby the pigs were anesthetized, intubated and ventilated. The CT scans were acquired on a Definition Dual Source CT scanner (Siemens). The 4DCT data set each consisted of twenty cardiac motion phases, the reference phase was motion phase zero. Nativ CT scans were recorded. In order to distinguish structures within the heart contrast enhanced CT scans were also aquired after the native scans. The radiopaque material was administered intravenously.

Segmentation of the target volumes as well as the OAR were carried out by a collaborating cardiologist at Mayo Clinic with Eclipse™(Varian Medical Systems). The volumes of the contours for the different ablation sites are presented for each pig in table 1.1. The location of these sites are visualized in figure 1.1 exemplary for pig 1. Contrary to humans pigs have only one PV pair, distinguished inbetween inferior PV (IPV) and superior PV (SPV). The contour for the PV encircles both of these structures.

Table 1.1: Target volume for the different cardiac target sites for all investigated pigs.

pig no	PVs [cm^3]	CTI [cm^3]	AV [cm^3]
1	0.72	0.20	0.08
2	1.01	0.13	0.05
3	1.09	0.24	0.06
4	1.03	0.31	0.02

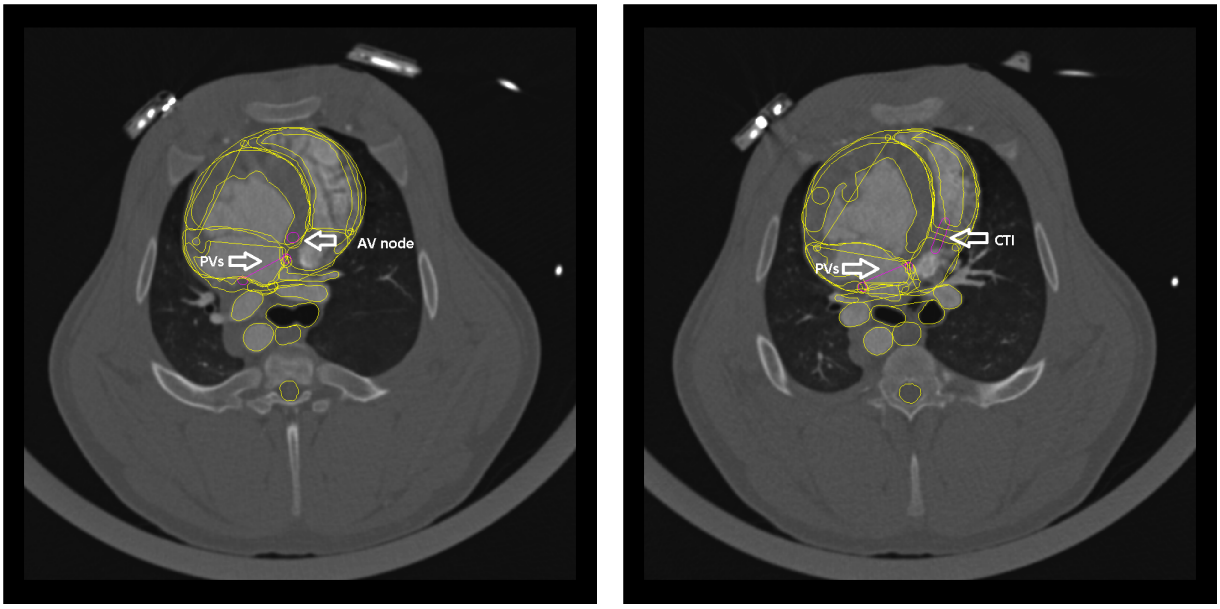

(a) PVs and AV node (b) PVs and CTI

Figure 1.1: Cardiac target volumes (PV, CTI and AV node) in pig 1.

Non-rigid image registration have been performed with Plastimatch [Sharp07] [Shack10]. A B-spline registration with the following parameters were chosen. For the contrast enhanced CT scans the regularization was chosen to λ=0.005, the first step was carried out with 50 maximal iterations and the spacing between the control points of the B-spline grid was chosen to 4mm in all three directions. In the second step, with 100 maximal iterations, the grid spacing was chosen to 1mm in all directions. For the native CT scans the grid spacing was the same, but the regularization lambda was chosen to λ=0.0001. The quality of registration was validated with visualization techniques: false color images [Bro07], checker board images [Bro07] as well as a qualitative check of the vector field regularization. These tests were carried out between motion phase 3 (which is the motion phase of the maximal displacement of the ventricle) and the reference phase (motion phase zero) or motion phase 18 (the motion phase of the maximal displacement of the atria) and the reference phase.

1.1.2 Treatment planning parameters

Treatment plans without motion (3D, static) as well as with motion (4D) were generated. For the dose optimization process, 3D treatment plans were generated to homogenously cover the CTVs, 4D treatment plans covered the ITV [Gra12]. Both CTV and ITV were studied with additional safety margins of 5mm. The grid spacing was chosen to 1mm in x and y direction, respectively. The spacing between the IESs were chosen to 3mm$_{H2O}$. A maximal contour extension of 1.1 times the focal spot size of 4mm was chosen as well as a distal contour fall off of 4mm$_{H2O}$. TRiP's 'all points divergent beam' algorithm was used to calculate the absorbed dose.

All treatment plans were generated as single field uniform dose (SFUD). In all simulations a physical dose of 25 Gy was applied in one fraction.

The generation of treatment plans is furthermore also dependent on the theoretically possible beam application. Spill lenght, shape and particle density are thus important factors. As the here presented simulations should study the feasibility of the planned experiments at GSI, the corresponding accelerator parameters have been used. Thereby a spill length of 2.2s is assumed. The pause in between spills is either 2.2s, when no energy change is required afterwards, or 3.2s when a energy change is needed. The spill shape is approximated by a Gaussian function. The particle intensities feasible at GSI vary between $2x10^6$ particles per spill and $2x10^8$ particles per spill. Inbetween these two extreme intensity levels, fifteen different intensity levels can be used. In the resulting treatment plan, the intensity steps are automatically chosen. A minimum particle number of 75.000 was chosen.

The dose was planned to be applied from two different beam channel directions. As no carbon ion gantry is available at GSI, the beam position was chosen as two lateral fields with a couch angles of -90° and 90°. With these opposing fields the treatment should be more robust against potential uncertainties like range differences. Due to the GSI specific beam output, the particles are applied at an angle of -2.203°, which was integrated in the treatment plans as a gantry angle.

As the reconstruction of the 4DCTs was based on the time scale a phase-based motion state detection was employed. In order to consider possible divergence in the heartbeat motion pattern of the pigs, different motion periods (0.7s and 0.5s) as well as different starting phases (0° and 90°) were used. The fast motion periods were chosen in order to account for the fast heartbeat of the pigs, which lay between 110 and 120 beats per minutes.

Besides the original volume of the CTV a safety margin has been added to the volumes of the treatment planning study. The margin was applied in order to account for theoretically possible deviations in between treatment planning and delivery, like slight positioning errors, changes between CT acquisition and treatment delivery etc. In confer with the radiologists from Mayo Clinic an isotropic safety margins of 5mm has been chosen, which will also be applied in the irradiation with photons. The ITV volumes used as the final target were generated from the original CTV contour as well as the CTV with margin, so that potential range variations were considered in the margins.

1.1.3 Treatment planning studies

On the basis of 3D treatment plans on the AV node the dose to enclosed OAR were studied. These were carried out on the CTV of all four pig data sets. Furthermore the 3D treatment plans were produced as reference values to the 4D cases, as it represents the ideal but not deliverable dose distribution. 4D plans were distinguished between an underlying motion without any compensation, resulting in interplay patterns, and with the application of rescanning as motion mitigation technique. For rescanning two different rescan numbers (10 and 15) were compared. Static, interplay as well as rescanning treatment plans for all pigs where carried out with the two stated beam entry channels, a safety margin of 5mm, the stated treatment planning parameters and the four stated motion trajectories. All treatment planning studies were carried out on contrast enhanced CT scans.

1.1.4 Analysis

Both the dose deposition in OAR as well as dose homogeneity in the target volume were studied. For the OAR dose-volume restriction in esophagus, trachea, aorta and the whole heart were compared to values from RTOG study protocols (see table 1.2). As further OAR cardiac substructures (ventricles and coronary arteries) were studied. Here the mean dose into the structures as well as the maximum point dose and the maximal irradiated volume (thus sum over all voxels of the organ which receive dose) were analyzed. In general, the median values of these parameters over all pigs were further calculated. Besides the second quartile (median, 50th percentile) also the third quartile (75th percentile) was assessed. For comparison of the resulting dose coverage in the target region dose-volume-histograms (DVHs) were studied. Furthermore motion-volume-histograms (MVHs) [Ric13] were generated displaying the relative displacement of every voxel of the investigated volume to the reference phase in all three motion directions. With these the resulting motion of the cardiac target sites due to heartbeat could be assessed. In particular, the motion assessable from the native CT scans were compared with the contrast enhanced motion information.

Table 1.2: Dose-volume limits for OAR.

OAR	Volume [cc]	Dose [Gy]	endpoint
Aorta / great vessels	10	31	Aneurysm
Esophagus	5	11.9	Stenosis / fistula
Heart	15	16	Pericarditis
Trachea	4	10.5	Stenosis / fistula

1.2 Results

In the following the results of the motion assessment due to heartbeat will be shown. Afterwards the dose to OAR when irradiating the AV node will be presented in detail. For the treatment planning study different dose analysis parameters will be presented and compared for different cases (static, interplay and rescanning).

1.2.1 Motion directions and magnitude

Treatment planning for particle therapy is carried out on native CT scans, as the Hounsfield units (HU) give information on the density of the structures and hence enable a calculation of the needed particle range. Nevertheless, as the heart is such a dense muscular structure, it was not certain if native CT scans would offer the needed contrast to assess the motion of substructures within the heart. Thus a comparison between motion assessments of the cardiac target volumes in native and contrast-enhanced CT scans will be presented for one porcine data set. Afterwards the motion of all target volumes (PVs, CTI and AV node) will be shown for all pigs.

Motion of cardiac target volumes in contrast enhanced versus native CT scans

Only one of the four porcine data sets (pig 3) offered identical CT slices between native and contrast enhanced data sets. For a fair comparison this data set was hence analyzed. Using the resulting deformation maps from deformable image registration the motion of the ablation sites of PVs, CTI and AV node were assessed in both scans. Motion volume histograms (MVHs) [Ric13] displaying the relative displacement of every voxel of the investigated volume to the reference phase in all three motion directions were generated. The mean and standard deviation of these displacement values in each motion phase are plotted for all motion directions in figures 1.2 - 1.4. It can be seen that the motion assassable in the contrast enhanced CT is much larger than in the native CTs. While the mean absolute displacement in the native CT is smaller than 1mm in case of PVs and AV node and smaller than 1.5mm in case of CTI, the contrast CT enables a motion assessment with yields a mean absolute displacement of larger than 2mm in all studied target volumes (see table 1.3). The difference is especially large in the AV node, a structure found in the center of the cardiac muscle. The maximal observable displacement for this structure in case of the native CT scan is (0.23 $\pm$ 0.08) mm (MP 12), while with the contrast enhanced CT an absolute displacement of (2.47 $\pm$ 0.37)mm is assassable in this motion phase and the maximal absolute displacement is found to (4.35 $\pm$ 0.10)mm (MP 5) (see Appendix XXX). It can thus be concluded that contrast enhanced CTs are needed in order to fully assess the motion of cardiac target volumes in pigs.

Table 1.3: Mean displacement of cardiac taget volumes in pig 3 over all motion phases.

	Target	ABS [mm]	SI [mm]	AP [mm]	LR [mm]
contrast CT	PVs	2.09 ± 0.61	0.27 ± 0.43	1.83 ± 0.69	-0.17 ± 0.73
	CTI	2.14 ± 0.46	0.81 ± 0.39	1.71 ± 0.47	0.01 ± 0.48
	AV	2.05 ± 0.39	0.45 ± 0.19	1.73 ± 0.32	-0.66 ± 0.43
	Target	ABS [mm]	SI [mm]	AP [mm]	LR [mm]
native CT	PVs	0.88 ± 0.44	0.03 ± 0.44	0.11 ± 0.51	-0.12 ± 0.52
	CTI	1.11 ± 0.50	-0.07 ± 0.59	0.61 ± 0.51	-0.09 ± 0.48
	AV	0.14 ± 0.06	0.05 ± 0.06	0.00 ± 0.07	0.00 ± 0.06

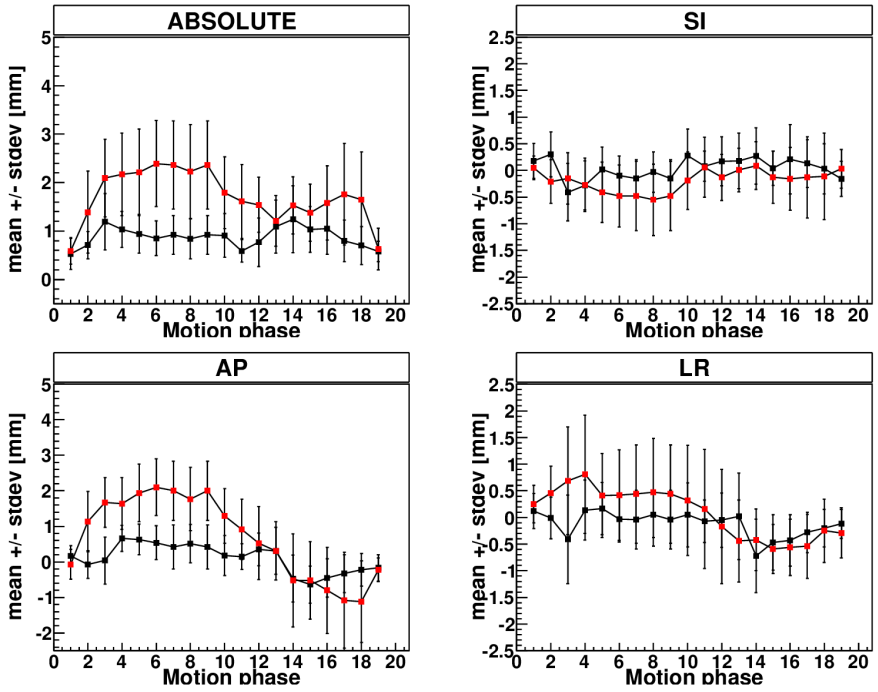

Figure 1.2: PV: motion amplitude in each motion phase of the heart beat relative to the reference phase. Comparison between nativee CT data (black) and contrast CT (red) for Pig 3.

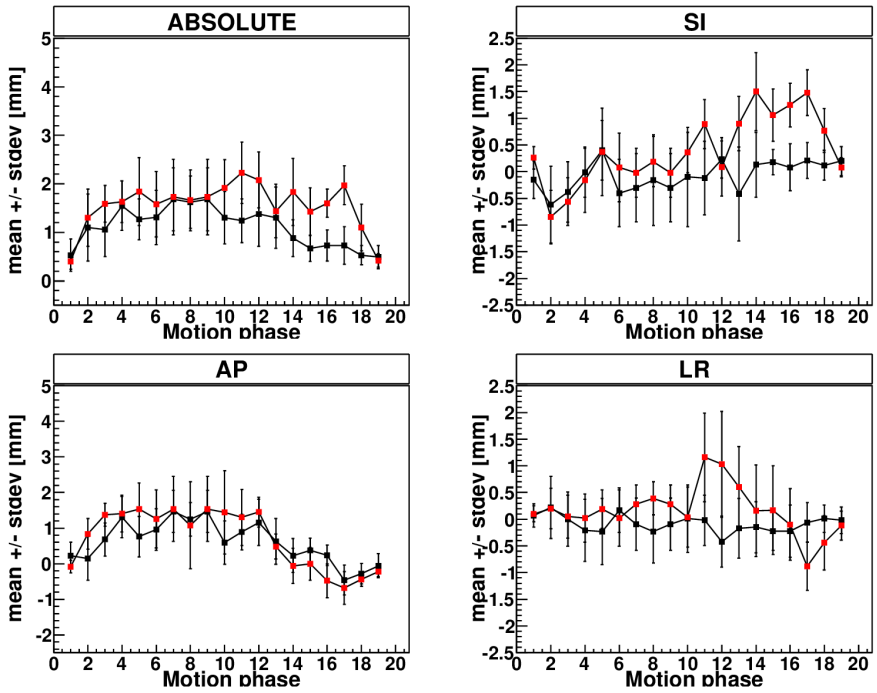

Figure 1.3: CTI: motion amplitude in each motion phase of the heart beat relative to the reference phase. Comparison between nativee CT data (black) and contrast CT (red) for Pig 3.

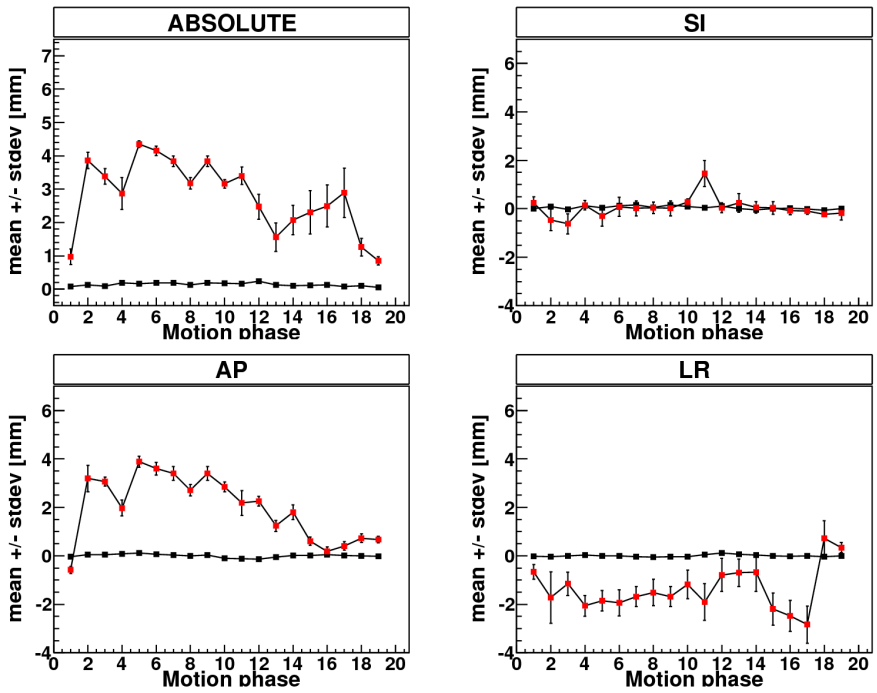

Figure 1.4: AV: motion amplitude in each motion phase of the heart beat relative to the reference phase. Comparison between nativee CT data (black) and contrast CT (red) for Pig 3.

The mean and standard deviation over all target volume voxels are plotted for each motion phase and for all pigs and motion directions in figure 1.5 to 1.7. It can be seen that the displacement within the cardiac target volume varies dependent on the studied pig and are hence dependent on the underlying anatomy. Furthermore the highest absolute displacement can be observed in different pigs, depending on the studied target volume. While the PVs move the most in pig 1 with a displacement of up to 5mm, pig 2 has the largest motion both in CTI and AV node (more than 6mm in both structures, respectively) (see also table 1.4). In this table it can furthermore be seen that the maximal absolute displacement varies depending on the studied volume. The CTI moves with a bigger amplitude than the other two target volumes, in three of the four studied pigs (difference found in pig 3). The smallest displacement is found in the PVs, again in three of the four studied data sets (again the difference is found in pig 3). This can be interpreted in connection to the placement of the target volumes within the heart. While the PVs are found in the upper atria, the CTI is located in the lower atria and hence the influence of the ventricular motion should be bigger. The AV node is in between the atria and ventricles and was found to have an intermediate absolute displacement in most cases (exception in pig 3). Independent of the studied target volume the largest contribution to the absolute displacement is found in AP direction for all pigs (see table 1.5). This can also be seen in the mean displacements over all pigs. For the PVs the mean amplitude in SI direction is (0.30 $\pm$ 0.77)mm, (1.53 $\pm$ 1.06) in AP direction and (-0.46 $\pm$ 0.95) in LR direction. In case of the CTI the mean amplitude in SI is (0.75 $\pm$ 0.74), (1.84 $\pm$ 0.65) in AP and (0.52 $\pm$ 0.85) in LR. For the AV node it is (0.71 $\pm$ 0.33) in SI, (2.42 $\pm$ 0.36) in AP and (-0.67 $\pm$ 0.47) in LR. On average, the absolute amplitude over all motion phases and pigs is found to (2.32 $\pm$ 0.79)mm for the PVs, (2.78 $\pm$ 0.68) for CTI and (2.97 $\pm$ 0.39)mm for the AV node.

It can moreover be seen in table 1.4 that no motion phase can be directly connected to the maximal absolute displacment of the target volumes. Since the motion phases of the heartbeat gated CT scan are based on the ECG trace and result in a division of a single heartbeat the motion phases should be directly assigned to the contraction (systole) and dilatation (diastole) of both atria and ventricles. Contraction of the atria (atrial systole) is occurring in between motion phase four and nineteen, in the same time as the ventricular relaxation (ventricular diastole). The ventricular systole and at the same time atria diastole are hence much shorter, occurring in the remaining motion phases twenty to three. The maximal displacement of the atria should thus be observed in motion phase eightteen, while the maximal amplitude of the ventricle should be observed in motion phase three. While this pattern is not directly connectable to the motion of the cardiac volumes it can nevertheless be seen that for all pig the displacement in the biggest motion direction (AP) results in a shallower motion in between MP 6 and 13 compared to the

other MPs. For the PVs the motion in pig 1 (pig with the largest motion in this target volume) has a range of less than 0.5mm in the interval between MP 6 and 13, while the motion ranges more than 3mm in the other MPs (see Appendix XXX). The same can be observed in case of the CTI, where pig 2 has a less shallow motion range of about 2mm within MP 6 and 13, but nevertheless a larger motion range of up to 4mm in the other MPs. Also for the AV node the motion within the MP interval (6-13) is lower (up to 2mm) compared to the the other MPs (range of about 4.5mm) in pig 2.

Table 1.4: Biggest absolute displacement of target volumes for all pigs with corresponding motion phase.

Target	Pig 1 [mm] (MP)	Pig 2 [mm] (MP)	Pig 3 [mm] (MP)	Pig 4 [mm] (MP)
PVs	4.22 ± 1.07 (13)	3.71 ± 1.55 (12)	2.39 ± 0.89 (06)	3.13 ± 1.03 (11)
CTI	5.79 ± 0.98 (07)	6.34 ± 0.54 (08)	2.23 ± 0.63 (11)	3.95 ± 0.83 (13)
AV	4.93 ± 0.26 (13)	6.04 ± 0.19 (11)	4.35 ± 0.10 (05)	3.63 ± 0.67 (10)

Table 1.5: Mean displacement of target volumes over all motion phases for all pigs and motion directions.

Target	Pig	ABS [mm]	SI [mm]	AP [mm]	LR [mm]
PVs	1	2.88 ± 0.74	0.24 ± 1.00	2.02 ± 1.28	-1.05 ± 1.11
	2	2.30 ± 0.94	0.85 ± 0.91	1.38 ± 1.16	-0.63 ± 1.02
	3	1.71 ± 0.78	-0.19 ± 0.55	0.68 ± 0.92	0.08 ± 0.81
	4	2.09 ± 0.61	0.27 ± 0.43	1.83 ± 0.69	-0.17 ± 0.73
	Pig	ABS [mm]	SI [mm]	AP [mm]	LR [mm]
CTI	1	3.54 ± 0.82	0.73 ± 0.84	2.30 ± 0.82	1.51 ± 0.92
	2	3.51 ± 0.78	0.96 ± 1.01	2.37 ± 0.54	0.31 ± 1.17
	3	1.55 ± 0.55	0.40 ± 0.50	0.70 ± 0.66	0.17 ± 0.57
	4	2.14 ± 0.46	0.81 ± 0.39	1.71 ± 0.47	0.01 ± 0.48
	Pig	ABS [mm]	SI [mm]	AP [mm]	LR [mm]
AV	1	2.96 ± 0.41	0.39 ± 0.42	2.54 ± 0.49	-0.70 ± 0.40
	2	3.70 ± 0.36	1.89 ± 0.34	3.04 ± 0.26	0.11 ± 0.36
	3	2.78 ± 0.37	0.04 ± 0.31	1.98 ± 0.27	-1.37 ± 0.61
	4	2.05 ± 0.39	0.45 ± 0.19	1.73 ± 0.32	-0.66 ± 0.43

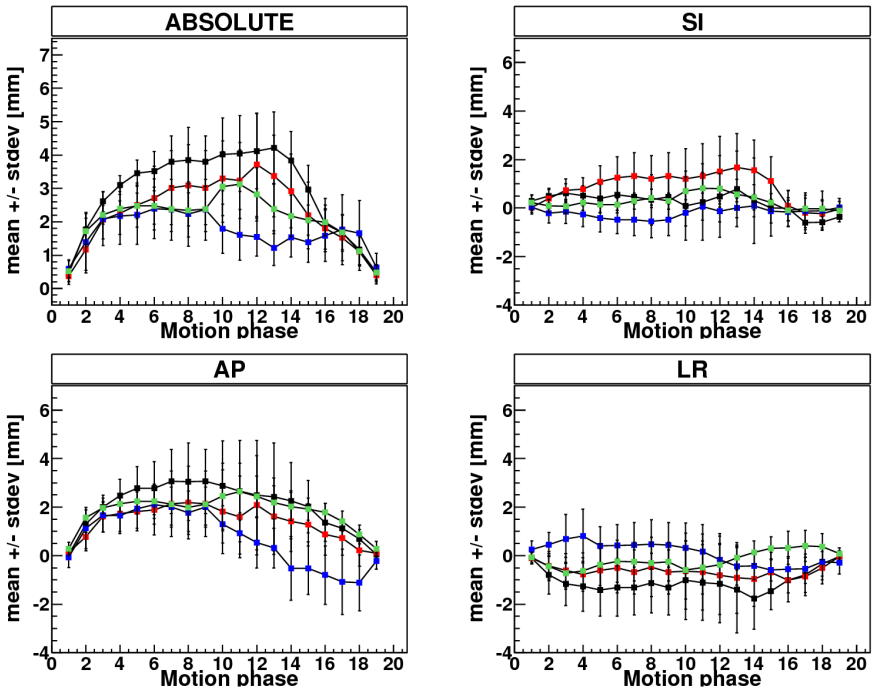

Figure 1.5: Motion amplitude of PVs under influence of heartbeat for all porcine. (pig 1: black, pig 2: red, pig 3: blue, pig 4: green)

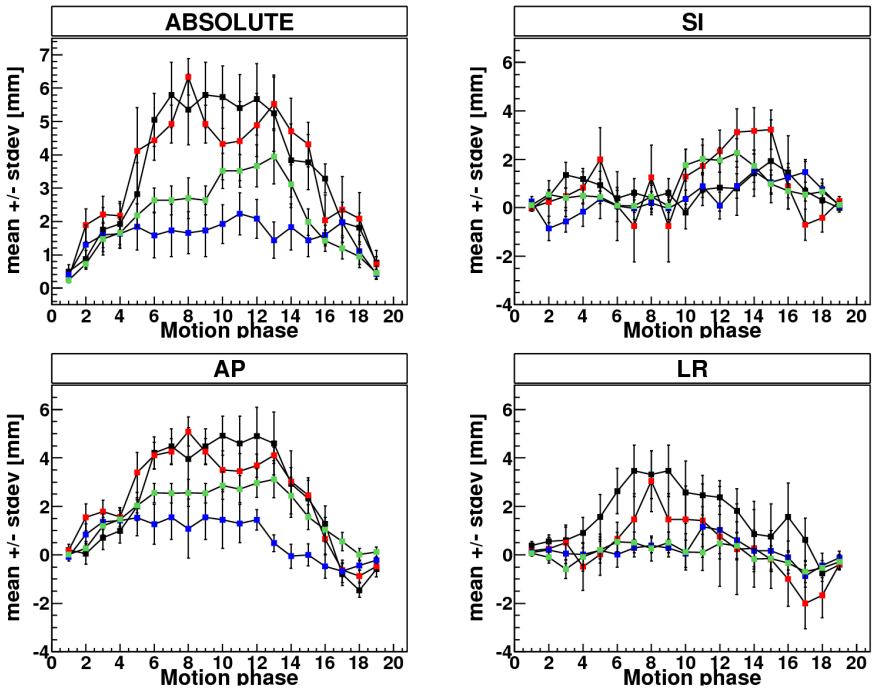

Figure 1.6: Motion amplitude of CTI under influence of heartbeat for all porcine. (pig 1: black, pig 2: red, pig 3: blue, pig 4: green)

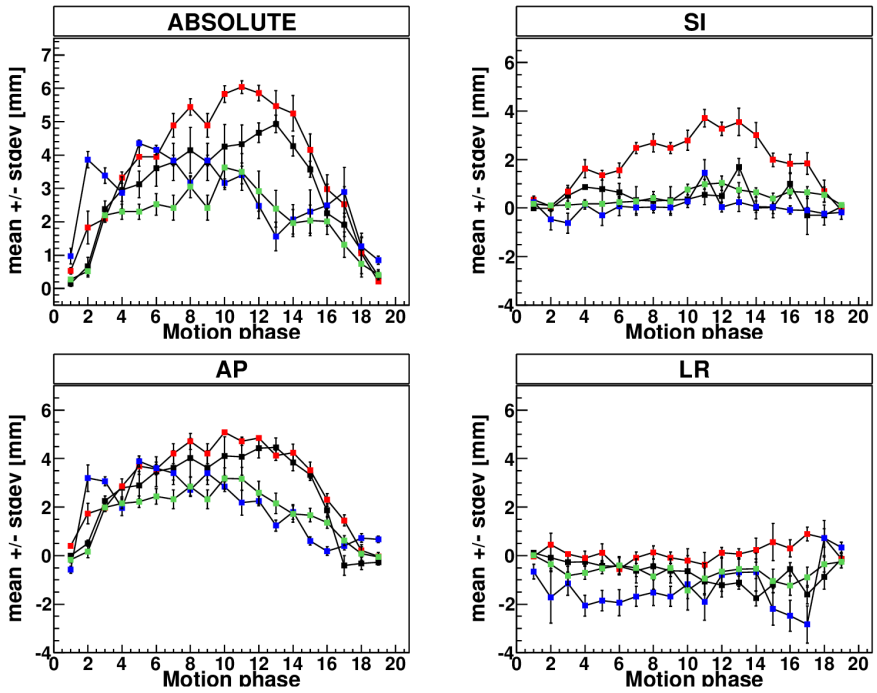

Figure 1.7: Motion amplitude of AV node under influence of heartbeat for all porcine. (pig 1: black, pig 2: red, pig 3: blue, pig 4: green)

The overall displacement field for two exemplary pigs with a small motion amplitude (pig 4) and a large motion amplitude (pig 2) of the AV node are shown in figure 1.8. The field is shown for the maximal displacement motion phase of the respective pigs (motion phase 11 for pig 2 and motion phase 10 for pig 4, see table 1.4). In order to visualize the location of the displacement, an axial cut of the reference state CT is underlayed. The absolute values of the displacement vectors are shown as contour plots.

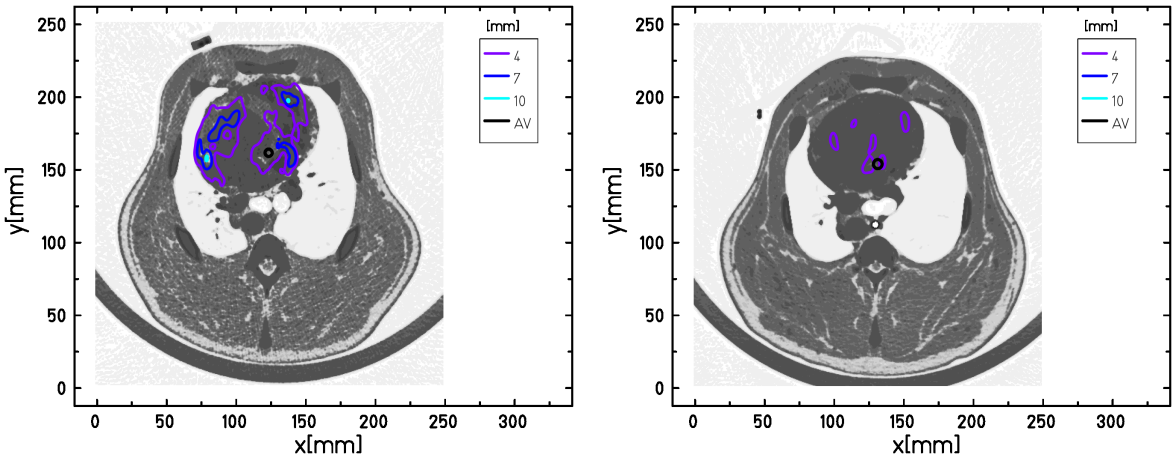

(a) Pig 2: max absolute motion (MP 11) (b) Pig 4: max absolute motion (MP 10)

Figure 1.8: Axial slices of the reference state of the CT overlayed with the absolute values of the displacement field (obtained from deformable image registration) in the corresponding slice for heartbeat motion. Left: the resulting displacement of pig 2 is shown in MP 11. Right: the results for pig 4 in MP 10.

1.2.2 Dose to organs at risk for the irradiation of AV node

Due to the fact that the AV node is located in a large distance to the OAR (see figure 1.1), the dose deposition in the studied structures is noncritical. The dose-volume limit results in the four studied porcine data sets can be seen in figure 1.9. Esophagus, trachea as well as the aorta are receiving no dose in all studied cases. Only the heart is receiving a certain dose deposition. Nevertheless the respective dose-volume limit, which is represented by a dashed line in the plot, is not endangered. The dose deposited in $15cm^3$ of heart ranges from 19% (pig 3) to 29% (pig 4) of the physical dose, thus even higher doses of up to 40Gy would not exceed the dose volume limit.

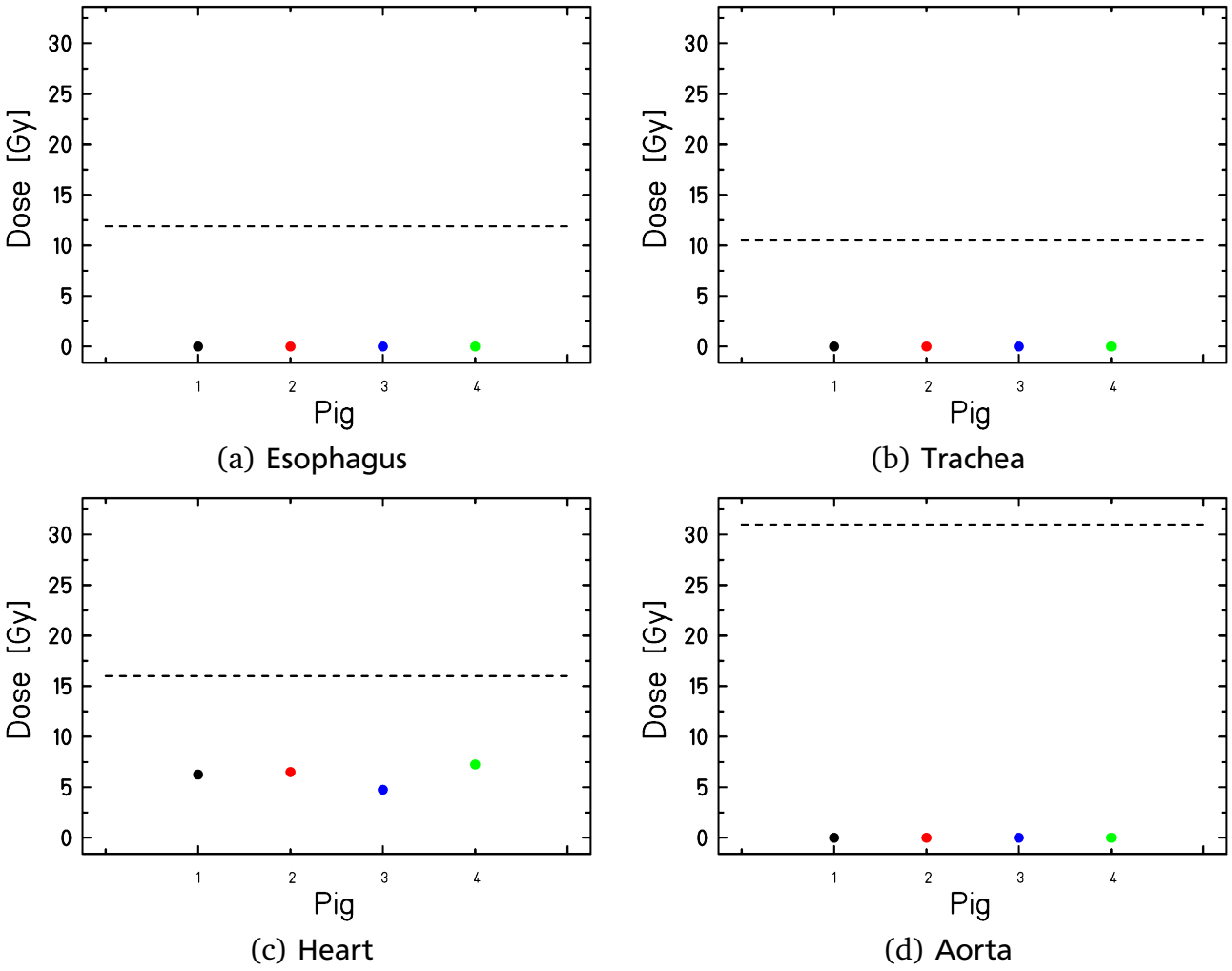

Figure 1.9: Dose-volume data of different OAR when irradiating the AV node in the four porcine data sets with a margin of 5mm. The dose-volume-limit for each critical organ is indicated with a dashed line in each plot, respectively.

The results of a more detailed analysis of the affected cardiac substructures can be seen in table 1.6. Here the mean dose to the whole structure is stated next to the maximal point dose for all pigs and studied structures. Furthermore the maximal irradiated volume is shown.

Table 1.6: Mean as well as maximum point dose to the whole heart and different critcal cardiac substructures as well as maximal irradiated volume of the structures for all pigs.

OAR	Pig	Mean dose [Gy]	Max dose [Gy]	Max volume [%]
Heart	1	0.6	25.8	14.0
	2	0.5	25.4	12.7
	3	0.8	25.3	17.4
	4	0.8	25.7	16.6
LV	1	0.5	26.3	6.7
	2	0.5	26.3	6.1
	3	0.3	26.1	5.1
	4	0.4	26.0	4.5
RV	1	0.3	25.2	9.1
	2	0.2	25.2	8.0
	3	0.4	25.3	9.6
	4	0.5	25.8	14.3
LCA	1	0.8	7.4	19.9
	2	0.6	7.2	13.5
	3	0.2	6.4	8.9
	4	0.7	7.4	14.6
RCA	1	1.5	9.2	37.6
	2	1.1	8.4	24.0
	3	1.4	9.8	37.3
	4	1.4	9.6	34.1

Due to the physical dose deposition of 25Gy in the AV node the heart is receiving a relatively high maximal point dose with a median of 25.6Gy (75th percentile: 25.8Gy) over all pigs. The mean heart dose is found to have a median of 0.7Gy (0.8Gy) and the median of the maximal irradiated volume over all porcine data sets is 15.3% (17.7%). Comparing the dose deposition in the left and right ventricles it can be seen that the maximum point dose is higher in the LV than in the RV, with a median of 26.2Gy (26.3Gy) compared to 25.2Gy (25.5Gy). Nevertheless the mean dose is comparable with a median of 0.5Gy (0.5Gy) for the LV and 0.4Gy (0.5Gy) for the RV and the maximal irradiated volume is smaller for the LV compared to the RV with a median of 5.6% (6.4%) compared to 9.3% (11.9 %). Concerning the coronary arteries it can be seen that the mean and maximal point dose to the LCA is smaller than to the RCA, resulting in a median mean dose of 0.6Gy (0.7Gy) in LCA compared to 1.4Gy (1.4Gy) in RCA and a median maximum point dose of 7.3Gy (7.4Gy) in LCA compared to 9.4Gy (9.7Gy) in LCA. Also the maximal irradiated volume is much smaller in the LCA compared to the RCA, resulting in a median maximum volume of 14.1% (17.2%) versus 35.7% (37.5%).

1.2.3 Motion mitigation techniques for AV node irradition

The absolute motion amplitudes of the AV node of up to 6mm due to heartbeat are expected to yield dose inhomogeneities when not compensated for. The resulting Interplay effect and dose deposition was studied for every porcine data set for different motion patterns and 5mm margin to the target volume. The dose analysis values V95, V107 and D5-D95 were assessed and plotted. For comparison also the corresponding values for the 3D case (static) are shown. Rescanning was studied as motion mitigation technique. The results of the stated dose values in case of rescanning with rescan numbers of ten and fifteen will be presented.

Dose deposition

A representative dose deposition for all studied techniques (static, interplay and rescanning with fifteen rescans) is shown exemplary for pig 2 (as this is the pig with the largest motion amplitude in the AV node) in figure 1.11. Rescanning and interplay are shown for a motion with a period of 0.5s and a starting phase of 90°. The target volume was irradiated with an added margin of 5mm. It can already been seen from this dose cut figures that rescanning with fifteen rescans improves the outcome compared to interplay and yields a result which is comparable to the static case. Due to the mechanism of rescanning, the field size is slighlty increased compared to the static irradiation.

For pig 2, the different motion patterns DVHs of fifteen rescans compared to the interplay results as well as a static irradiation are displayed in figure 1.10 for 5mm safety margin. In order to assess the dose information of all patients the DVHs were analyzed and compared for dose steepness, dose coverage as well as over dosage. The results for all porcine data sets can be seen in figure 1.12. The corresponding numerical values can be found in appendix XXX (tables 1.21 - 1.24).

As can be seen from figure 1.12 the resulting interplay pattern is dependent on the underlying motion period and starting phase. This can also be seen in the mean values and standard deviations of the dose analysis parameters over all patients for different motion patterns. The dose coverage for example is found to have a mean value of V95=(84.3 $\pm$ 17.5)% for a motion with 0.7s period and a starting phase of 0°, while it is found to (91.0 $\pm$ 10.3) for the same period and a starting phase of 90°. For a period of 0.5s the mean dose coverage over all pigs is found to (84.5 $\pm$ 8.0) with a phase of 0° and to (86.0$\pm$ 24.0) for a phase of 90°. The resulting high standard deviation shows that the result is also dependent on the studied porcine case. These dependencies are also valid for the other studied dose analysis parameters, dose homogeneity and over dosage.

It can furthermore be seen in figure 1.12 (as well as numerical values for all pigs in appendix XXX) that rescanning can improve the results for dose steepness, dose coverage as well as over dosage compared to the interplay case in all studied motion cases for three out of four pigs. Pig 2 on the other hand, who was found to have the largest absolute displacement of the AV node out of the four studied porcine data sets, results in some cases where rescanning yields slighlty inferior results compared to interplay. This is the case in dose steepness, where a motion with 0.7s and 90° starting phase results to D5-D95=7.9% with ten rescans compared to D5-D95=6.2% without any compensation (interplay). For the same motion the dose coverage is found to V95=98.5% with ten rescans compared to V95=99.0% with interplay. Also in over dosage a motion pattern (period of 0.5s and starting phase of 0°) is found to result in inferior results compared to interplay (9.31% versus 0%). Nevertheless these results could be improved with fifteen rescans, so that e.g. the dose coverage is found to V95=100% for the stated motion pattern (0.7s period and 90° starting phase) (static: 100%), hence resulting in an improved result compared to interplay and even reaching the static irradition. For pig 4, who has the smallest absolute displacement of the AV node in the studied porcine cohort, all rescanning results yield improved results compared to interplay. Nevertheless it can also here be observed that fifteen rescans results in better dose analysis parameters and even improves the static outcome in some cases. E.g. the dose steepness is found to D5-D95=3.0% with a motion period of 0.5s and starting phase of 0° for fifteen rescans and to 5.1% with ten rescans, while in the static case it is found to 5.5%. For the dose coverage fifteen rescans yields results as he static result (100%) for all motion patterns, while ten rescans yields slighlty inferior results (e.g. 97.8% for motion period of 0.7s and starting phase of 90°, interplay: 74.3%).

As the dose coverage is especially important for the planned experiments in order to to enable a correct dose-escalation study fifteen rescans are hence favorable. For the here studied motion pattern and porcine data set cases this rescan number would lead to a dose deposition corresponding to the planned dose deposition.

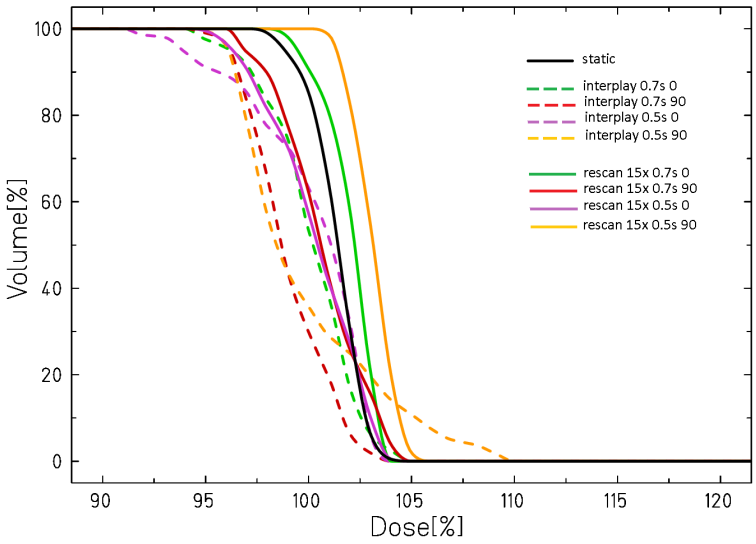

(a) pig 2

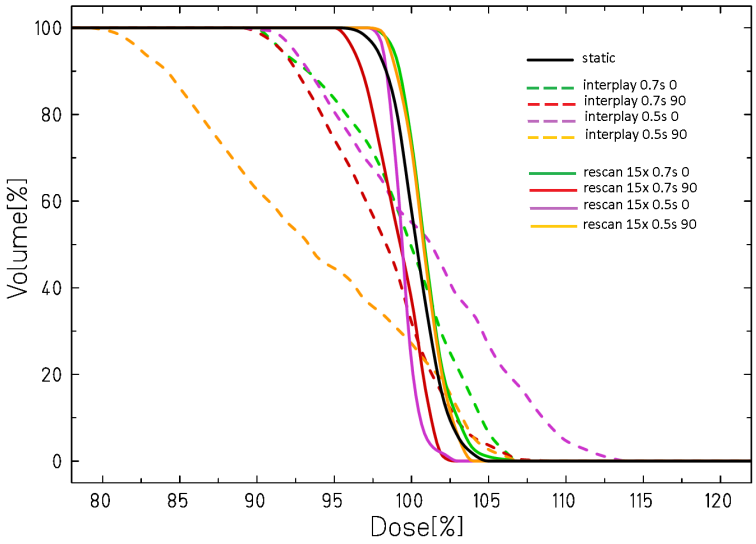

(b) pig 4

Figure 1.10: Dose volume histograms for CTV of pig 2 (largest absolute displacement of AV node) and pig 4 (smallest absolute displacement of AV node) for 5mm safety margin irradiation of AV node in case of static irradiation (black), interplay (dashed) and rescanning with fifteen rescans (solid). The motion patterns are shown in colors (0.7s 0: motion period of 0.7s and starting phase 0°, 0.7s 90: motion period of 0.7s and starting phase 90°, 0.5s 0: motion period of 0.5s and starting phase 0°, 0.5s 90: motion period of 0.5s and starting phase 90°).

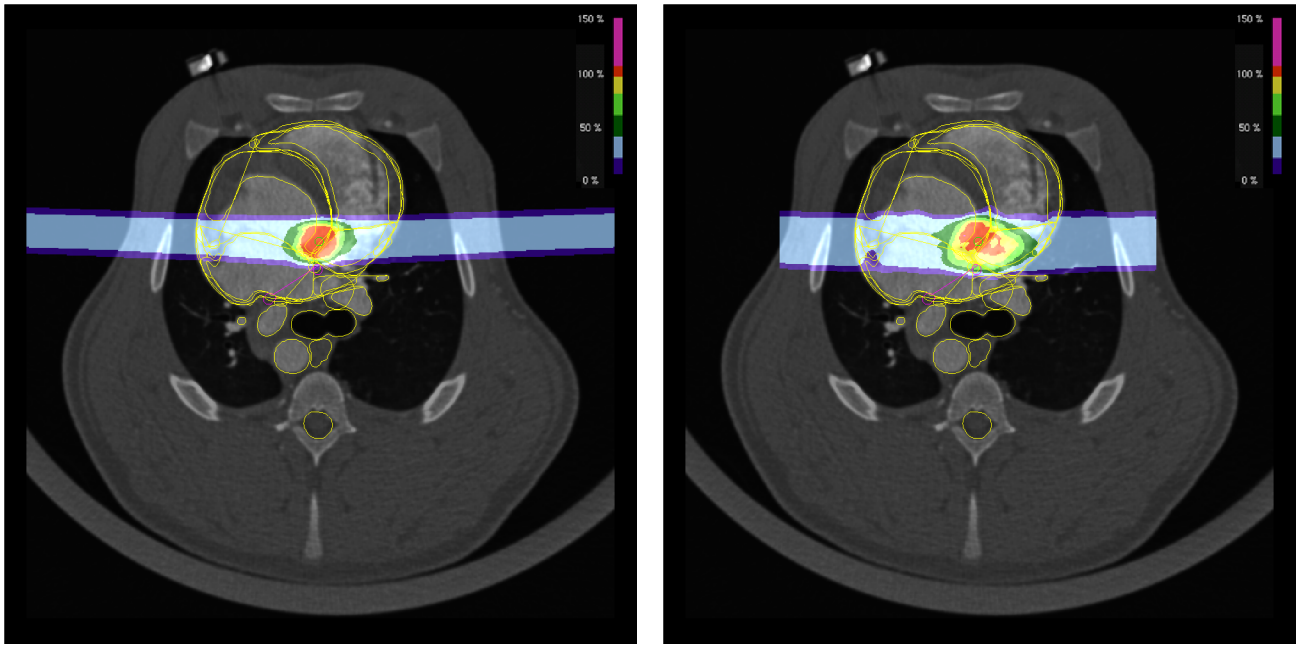

(a) static (b) interplay

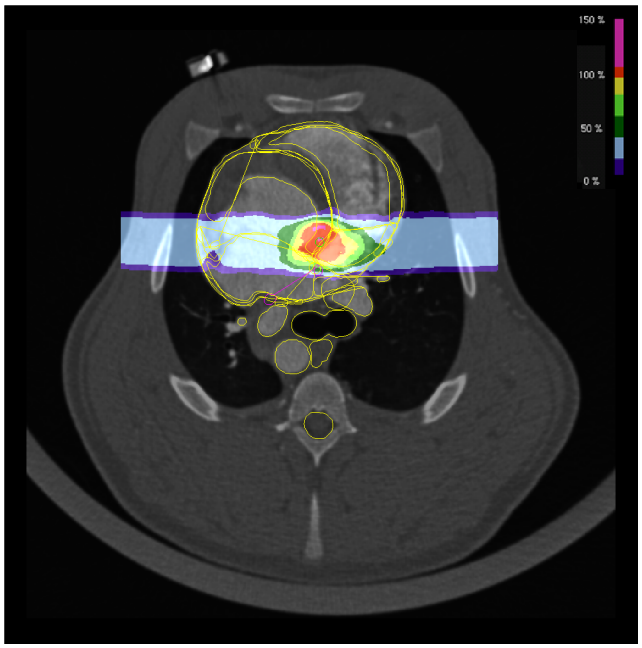

(c) rescanning (15x)

Figure 1.11: Dose distribution of pig 2 for static (a) as well as interplay (b) and fifteen rescans (c) at motion period of 0.5s and a motion starting phase of 90°. The target volume has an added margin of 5mm. The improved outcome of rescanning compared to interplay can already be seen in these dose cuts. The window size for interplay and rescanning have been reduced in the simulations.

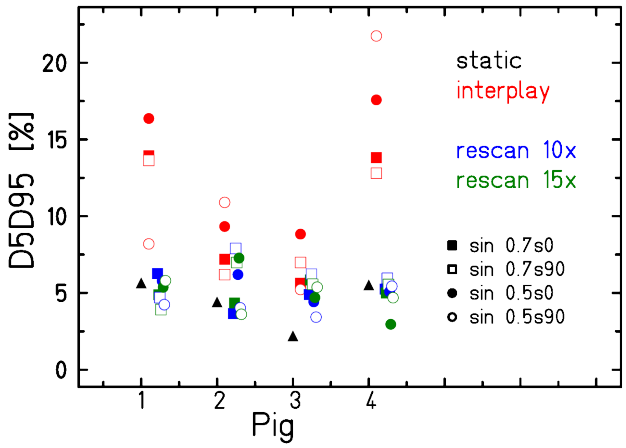

(a) D5-D95

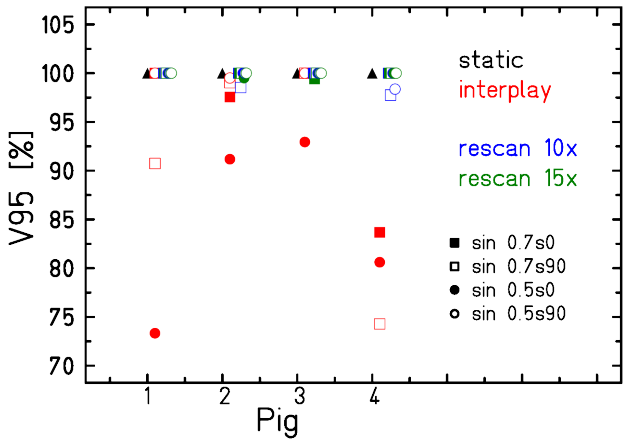

(b) V95

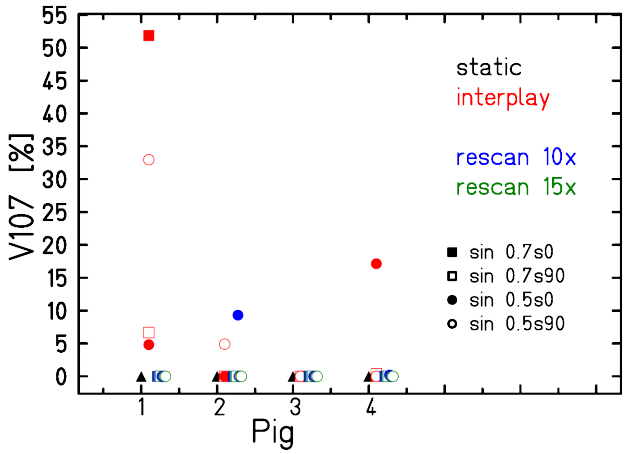

(c) V107

Figure 1.12: Dose analysis parameters D5-D95 (first row), V95 (middle row) and V107 (last row) for all porcine data sets when irraditing the AV node with 5mm safety margin. Static (black) as well as interplay (red) and different rescanning numbers (10 times: blue, 15 times: green,) were compared for different motion patterns and safety margins. For a better visualization the rescanning data points for each motion pattern are shifted.

In figure 1.13 the irradiation time for rescanning of AV node are shown for all pigs and the two studied beam channel directions (couch angle 90° and -90°). The stated results were achieved with a low intensity irradiation (minimal particle number of 5.000). For an irradiation with 5mm margin the treatment time over all pig data sets results to a mean value of about one minute per field (see table 1.7). Thus the overall treatment time would result to (1.85 ± 0.12)min with rescanning as motion mitigation technique for heartbeat motion in porcine data. Theoretically, this result could be further reduced with a higher minimum particle number and hence a higher irradiation intensity. Nevertheless these irradiation times are already very short due to the small target volume. It needs to be observed in the upcoming experiments if these short treatment times can be verified.

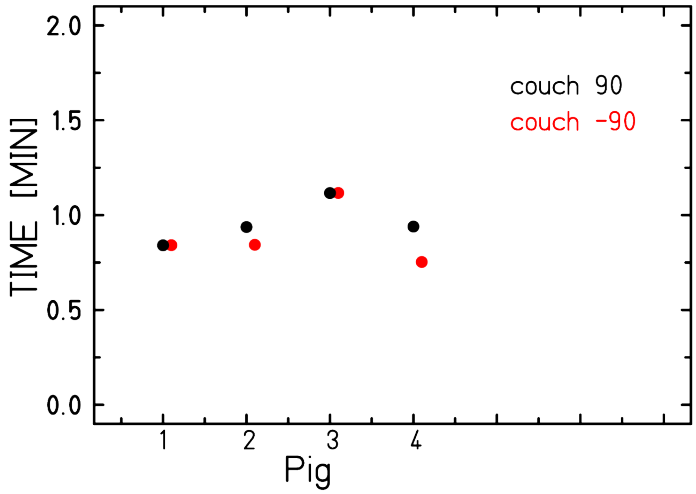

Figure 1.13: Irradiation time of fifteen rescans for all pigs and beam entry channels.

Table 1.7: Mean irradiation time for AV node with a safety margin of 5mm over all pigs.

Couch angle [°]	time [min]
-90	0.89 ± 0.14
90	0.96 ± 0.10
total	1.85 ± 0.12

1.3 Discussion

In this chapter the influence of heartbeat motion on different cardiac target volumes (PVs, CTI, AV node) in porcine data sets were studied and treatment planning studies with rescanning as motion mitigation technique were carried out. A detailed analysis of the dose depositions to the OAR was performed, with special emphasis on the irradiation of cardiac substructures. This analysis is motivated by the planned experiments on the feasibility of the non-invasive ablation of cardiac target sites with carbon ions. These experiments will be carried out in animal models. In experimental cardiology dogs as well as pigs are most frequently used. As dogs are known to display certain differences in anatomy and physiology compared to man [Hug86] [Cri98] it is planned to use pigs in the upcoming GSI experiments.

Even though it seems to be accepted in literature that the anatomy of pig hearts are very similar to that of humans [Lum66] [Dou72] [Hug86] [Coo91] [Whi93] Crick et al. [Cri98] carried out a detailed comparison between the anatomy of porcine and human hearts. They found several significant differences which they suspected to arise mainly from the different orientation of the bodys (unguligrade versus orthograde) and hence location of the heart in the thorax and from the differing form of the thorax itself. While the upper and lower borders of the hearts were found to have similar size and features, the general shape differs as the pig hearts are more 'Valentine' shaped and the human hearts more trapezoidal. This also leads to important differences in the internal anatomy. While in human hearts the right atrium is typically larger than the left, the atria of pigs have a similar size. Concerning the left atrium only two orifices for the pulmonary veins are observed, while in human hearts four pulmonary vein openings can be located. The right atrium was furthermore stated to differ significantly from the human heart, especially in the atrial appendage. Regarding the ventricles Crick et al. stated that the right ventricle was observed to have a similar structure than human hearts, such as the tricuspid and pulmonary valvar arrangements. But also here differences were found (e.g. the orientation of the pulmonary valve). The left ventricles seem to have similar features to the human structure, but the ventricular wall was found to be much thicker in porcine. Furthermore it was stated that the left chambers of the pig hearts were significantly bigger compared to the right chambers, so that the apex was found to be composed entirely of left ventricular musculature. In human hearts the chambers are usually equal in size. Concerning coronary circulation it was noted that most pigs displayed a blood supply to the sinus and atrioventricular node by branches of the right coronary artery, while in humans this is observed to a lesser extend.

Due to the different anatomy of pigs compared to humans it was expected to find different results in the motion of the cardiac target volumes as well as in the dose deposition to the OAR. The findings will be discussed in the next subsections.

1.3.1 Movement of cardiac target volumes in cardiac cycle

Due to the dense muscular structure of the heart contrast enhanced CT scans were acquired in comparison to native scans. Deformable image registrations were carried out on both data sets and the resulting motion displacement of the cardiac target volumes were assessed. It could be concluded that native CT scans do not enable an estimation of either the motion amplitude or direction. While e.g. the mean absolute displacement of the AV node was found to (0.14 $\pm$ 0.06)mm in the native scans of pig 3, the mean absolute displacement on contrast CT scans was found to (2.05 $\pm$ 0.39)mm. This difference is sufficient to completely alter the results of the treatment planning study as an interplay pattern would be expected with the motion field from the contrast enhanced CT scans, while the motion of the native scans would be too small to yield an interplay effect. It is thus obvious that contrast enhanced CT scans are needed in order to correctly assess the motion of the cardiac target volumes. As contrast enhanced CT scans change the Hounsfield unit information, which are needed for range informations in particle therapy, it is not intented to deliver treatment plans created on these data sets. In the case of treatment planning studies for pure feasibility it can nevertheless be accepted as the range information does not need to be applied. In the planned experiments at GSI a strategy to use the motion displacement field of the contrast enhanced CT, while carrying out the treatment planning on native CT scans, is nevertheless needed. A first concept could be to enable a robust stabilization of the pigs during CT acquisition so that no position divergence between the native CT scan and the injection of the contrast agent is induced. This would hence enable a direct application of the deformation field of the contrast enhanced CTs on the native CT scans.

Based on the contrast enhanced CT scans the motion of the cardiac target volumes - PV, CTI and AV node - in all four porcine data sets was assessed. It could be observed that the CTI moved the most in all four pigs, followed by the AV node. The PV moved to a lesser extend in all four pigs. It was assumed that these findings were connected to the location of the target volumes within the heart, where the PVs are found in the upper atria and the CTI in the lower atria, hence increasing the influence of the stronger ventricular motion. As the AV node is found in between ventricles and atria it can be hypothesized that the position is more stable and hence the influence of the ventricular motion on the displacement of the structure is slighlty reduced. Furthermore it was found that in all four porcine data sets as well as for all three studied cardiac target volumes the displacement in AP direction was larger than in the other two motion directions (SI and LR). For the porcine data sets a shallower motion range of the target volumes was furthermore observed in-between MP 6 and 13, enabling a potential application of gating as another motion mitigation technique for the compensation of heartbeat motion in swines. Nevertheless a close analysis of the individual motion pattern of the respective pig is needed as the motion differed in-between the animals.

1.3.2 Dose to critcal structures

Due to a lack of corresponding data dose-volume limits for the studied OAR (esophagus, trachea, aorta and heart) were taken from the RTOG protocols for SBRT treatments of humans. These limits were not exceeded in the irradiation of AV node with 5mm safety margin. It can be argued that this is due to the large distance of the target volume from the analyzed critical structures. Nevertheless the resulting dose deposition with carbon ions is also smaller than the results for photon irradiation. A study by radiologists from the collaborating Mayo Clinic [Son14] stated that an IMRT irradiation of the AV node with 5-6mm margin and (32 $\pm$ 0.6)Gy in the same porcine data sets resulted in a mean dose to the esophagus of 1.6Gy. In case of carbon ions no dose deposition was found in this structure (mean: (0 $\pm$ 0)Gy). The mean dose to the trachea was found to 2.2Gy with IMRT delivery, while also here no dose was deposited with carbon ions (mean: (0 $\pm$ 0)Gy). This result was found primary as 0% of the physical dose, so that the apparent discrepancy between the deposited physical dose in IMRT and carbon ions plans can be neglected. The finding would also hold true for a higher physical dose of e.g. 32Gy. Concerning the mean overall cardiac dose it was stated that an IMRT delivery would result in (4.7 $\pm$ 1.3)Gy. For carbon ions a mean cardiac dose of (0.03 $\pm$ 0.00)% of the physical dose was found, resulting in (0.7 $\pm$ 0.1)Gy for 25Gy or (1.0 $\pm$ 0.1)Gy for 32Gy, respectively. The better sparing of the critical structures with carbon ions compared to IMRT is one hand due to the reduced beam channel number. On the other hand the physical advantages of carbon ions compared to photon delivery (e.g. Bragg peak) become obvious in this results. The study by Song et al. also included an analysis of the dose deposition when irradiating the AV node with proton beams. Here a single AP field was applied, resulting in (30.7 $\pm$ 0.2)Gy to the AV node. The mean overall cardiac dose was stated to result to (3.6 $\pm$ 1.5) Gy. The dose deposition to the surrounding heart is hence higher in case of proton irradiation compared to carbon ions. This is especially striking since only one field was used in proton treatment compared to the here presented two carbon ion beam channels, hence resulting in a bigger irradiated cardiac volume. Nevertheless it should be kept in mind that the beam channels can not be directly compared, since two lateral fields were used in carbon ion treatment planning, while an AP field was applied in proton therapy.

The dose deposition in the cardiac substructures were also studied in the here presented AV node irradiation with carbon ions. The LV resulted to receive a slighlty higher maximum point dose compared to the RV, while the mean dose in the two structures were comparable and the maximal irradiated volume was smaller for the LV compared to the RV. In the study by Crick et. al is stated that the LV is significantly bigger compared to the RV in swines and that sensitive structures like the apex are composed entirely of LV musculature [Cri98]. It can thus be understood why the maximal irradiated volume of the LV is significantly smaller than the RV even

though the beam channels are symmetrical in lateral position. Concerning the coronary arteries it was found that the mean and maximal point dose to the LCA is smaller than the RCA and also the maximal irradiated volume of the LCA is smaller compared to the RCA. Since no dose limit information exist it is unclear whether the larger exposure of the RCA compared to LCA is problematic, especially since pigs were found to supply the SA and AV node via branches of the RCA.

1.3.3 Rescanning as motion mitigation technique

In the irradiation of cardiac volumes in the animal study carried out at CyberHeart and at the Universitätsklinikum Schleswig-Holstein in Lübeck, both with photons, only an ITV approach was used in order to compensate for heartbeat motion. Due to the interference effects between the active carbon ion beam application and the assessed motion of up to 6mm of the AV node due to heartbeat, a different approach was needed for carbon ions. Rescanning was studied as potential motion mitigation technique for the non-invasive ablation of the AV node with an underlying heartbeat motion in swines.

It was found that rescanning yields good dose analysis parameters. The dose coverage was higher than 99% in 93.75% of all studied cases and even increased to 100% of the studied cases when only fifteen rescans were analyzed. V107 values higher than 0% were obtained in 93.25% of all cases, which reduced to 0% of the studied cases when only the DVHs for fifteen rescans were evaluated. The dose homogeneity D5-D95 did not exceed 7.9%. This value was achieved with ten rescans and could be improved to 7.0% with fifteen rescans. It can thus be concluded that rescanning with fifteen rescans yields a slighlty better results. Especially the dose coverage, which is of particular interest for the planned feasibility study in animal models and the included planned dose escalation study, did improve with a slightly higher rescan number of fifteen rescans.

1.4 Conclusion

Contrast enhanced CT scans are needed in order to assess the motion of cardiac target volumes due to heartbeat motion. Potential cardiac target volumes in swine move due to heartbeat with an amplitude of up to a couple of millimeters and the dominant motion direction was found to be in AP direction. The displacement of the AV node creates interplay effects when irradiated with carbon ions. Rescanning as motion mitigation technique was studied. Rescanning with fifteen rescans yields improved dose analysis parameters compared to interplay in all studied pig cases and for all underlying motion patterns. It is thus an adequate motion mitigation technique for the planned experimental validation in animal models where the AV node will be irradiated. Dose-volume limits to the surrounding OAR were not exceeded.

for APPENDIX

Motion of target volumes in constrast enhanced CT scans

Table 1.8: PV: Mean and standard deviation of target motion in all phases of the heart beat, relative to the reference phase. The values are taken from the contrast CTs of Pig 1.

motion phase	ABS [mm]	SI [mm]	AP [mm]	LR [mm]
01	0.43 ± 0.23	0.30 ± 0.25	0.03 ± 0.13	-0.10 ± 0.24
02	1.76 ± 0.52	0.49 ± 0.28	1.29 ± 0.33	-0.79 ± 0.79
03	2.61 ± 0.30	0.62 ± 0.39	2.00 ± 0.49	-1.16 ± 0.89
04	3.10 ± 0.28	0.51 ± 0.41	2.47 ± 0.68	-1.27 ± 1.03
05	3.46 ± 0.39	0.40 ± 0.57	2.77 ± 0.90	-1.42 ± 1.07
06	3.52 ± 0.59	0.54 ± 0.64	2.78 ± 1.09	-1.31 ± 1.19
07	3.80 ± 0.77	0.46 ± 0.86	3.06 ± 1.32	-1.32 ± 1.12
08	3.85 ± 0.98	0.34 ± 1.04	3.04 ± 1.60	-1.13 ± 1.23
09	3.80 ± 0.77	0.46 ± 0.86	3.06 ± 1.32	-1.32 ± 1.12
10	4.02 ± 1.09	0.10 ± 1.42	2.88 ± 1.85	-1.01 ± 1.62
11	4.04 ± 1.14	0.25 ± 1.57	2.66 ± 2.09	-1.11 ± 1.56
12	4.12 ± 1.13	0.48 ± 1.68	2.49 ± 2.25	-1.16 ± 1.61
13	4.22 ± 1.07	0.79 ± 1.56	2.42 ± 2.22	-1.40 ± 1.79
14	3.83 ± 0.88	0.31 ± 1.76	2.26 ± 1.58	-1.77 ± 1.26
15	2.97 ± 0.72	-0.00 ± 1.16	2.02 ± 1.08	-1.46 ± 0.77
16	1.94 ± 0.76	-0.01 ± 0.75	1.37 ± 0.79	-1.01 ± 0.53
17	1.67 ± 0.55	-0.60 ± 0.43	1.12 ± 0.37	-0.79 ± 0.72
18	1.17 ± 0.46	-0.58 ± 0.30	0.69 ± 0.39	-0.34 ± 0.65
19	0.48 ± 0.23	-0.36 ± 0.20	0.05 ± 0.24	-0.04 ± 0.23

Table 1.9: CTI: Mean and standard deviation of target motion in all phases of the heart beat, relative to the reference phase. The values are taken from the contrast CTs of Pig 1.

motion phase	ABS [mm]	SI [mm]	AP [mm]	LR [mm]
01	0.49 ± 0.21	-0.02 ± 0.13	0.20 ± 0.23	0.39 ± 0.16
02	0.87 ± 0.26	0.46 ± 0.24	0.04 ± 0.43	0.55 ± 0.28
03	1.75 ± 0.66	1.35 ± 0.53	0.70 ± 0.48	0.61 ± 0.54
04	1.92 ± 0.62	1.18 ± 0.45	0.99 ± 0.51	0.91 ± 0.63
05	2.82 ± 0.94	0.93 ± 0.57	2.00 ± 0.58	1.56 ± 0.93
06	5.05 ± 0.80	0.39 ± 0.45	4.20 ± 0.66	2.63 ± 0.93
07	5.79 ± 0.98	0.62 ± 0.58	4.48 ± 0.73	3.47 ± 1.06
08	5.36 ± 1.06	0.42 ± 0.60	3.95 ± 1.31	3.31 ± 0.99
09	5.79 ± 0.98	0.62 ± 0.58	4.48 ± 0.73	3.47 ± 1.06
10	5.73 ± 0.94	-0.20 ± 0.66	4.92 ± 0.81	2.58 ± 1.29
11	5.40 ± 1.01	0.75 ± 0.65	4.60 ± 1.13	2.46 ± 0.82
12	5.67 ± 1.07	0.84 ± 0.98	4.90 ± 1.20	2.37 ± 0.70
13	5.25 ± 1.14	0.80 ± 1.11	4.60 ± 1.30	1.82 ± 0.91
14	3.83 ± 1.10	1.43 ± 0.95	2.92 ± 1.38	0.86 ± 1.35
15	3.78 ± 0.83	1.92 ± 1.71	2.32 ± 0.76	0.76 ± 1.35
16	3.29 ± 0.44	1.46 ± 1.52	1.28 ± 0.74	1.56 ± 1.40
17	1.97 ± 0.60	0.70 ± 1.30	-0.80 ± 0.47	0.62 ± 0.90
18	1.82 ± 0.43	0.31 ± 0.71	-1.46 ± 0.30	-0.76 ± 0.33
19	0.76 ± 0.37	-0.01 ± 0.17	-0.60 ± 0.32	-0.40 ± 0.23

Table 1.10: AV node: Mean and standard deviation of target motion in all phases of the heart beat, relative to the reference phase. The values are taken from the contrast CTs of Pig 1.

motion phase	ABS [mm]	SI [mm]	AP [mm]	LR [mm]
01	0.15 ± 0.09	-0.01 ± 0.06	-0.01 ± 0.04	0.12 ± 0.10
02	0.66 ± 0.27	-0.01 ± 0.14	0.51 ± 0.12	-0.08 ± 0.46
03	2.38 ± 0.24	0.52 ± 0.31	2.25 ± 0.21	-0.28 ± 0.41
04	2.95 ± 0.34	0.87 ± 0.11	2.80 ± 0.37	-0.25 ± 0.18
05	3.12 ± 0.40	0.79 ± 0.60	2.90 ± 0.56	-0.42 ± 0.21
06	3.60 ± 0.53	0.64 ± 0.38	3.46 ± 0.62	-0.44 ± 0.36
07	3.79 ± 0.56	0.33 ± 0.55	3.62 ± 0.70	-0.63 ± 0.50
08	4.14 ± 0.69	0.29 ± 0.39	4.03 ± 0.80	-0.44 ± 0.56
09	3.79 ± 0.56	0.33 ± 0.55	3.62 ± 0.70	-0.63 ± 0.50
10	4.25 ± 0.66	0.36 ± 0.33	4.10 ± 0.80	-0.64 ± 0.63
11	4.33 ± 0.57	0.54 ± 0.39	4.08 ± 0.76	-1.06 ± 0.56
12	4.67 ± 0.29	0.49 ± 0.40	4.43 ± 0.41	-1.21 ± 0.50
13	4.93 ± 0.26	1.70 ± 0.35	4.46 ± 0.39	-1.11 ± 0.27
14	4.27 ± 0.30	0.00 ± 0.44	3.84 ± 0.34	-1.76 ± 0.31
15	3.57 ± 0.24	0.03 ± 0.42	3.33 ± 0.23	-1.20 ± 0.15
16	2.25 ± 0.21	1.00 ± 0.46	1.86 ± 0.28	-0.56 ± 0.27
17	1.91 ± 0.35	-0.30 ± 0.78	-0.41 ± 0.40	-1.61 ± 0.38
18	1.14 ± 0.40	-0.29 ± 0.41	-0.32 ± 0.25	-0.88 ± 0.51
19	0.37 ± 0.15	0.06 ± 0.06	-0.27 ± 0.12	-0.14 ± 0.22

Table 1.11: PV: Mean and standard deviation of target motion in all phases of the heart beat, relative to the reference phase. The values are taken from the contrast CTs of Pig 2.

motion phase	ABS [mm]	SI [mm]	AP [mm]	LR [mm]
01	0.37 ± 0.25	0.02 ± 0.27	0.14 ± 0.20	-0.10 ± 0.24
02	1.16 ± 0.69	0.40 ± 0.42	0.78 ± 0.58	-0.43 ± 0.60
03	2.06 ± 0.57	0.73 ± 0.47	1.61 ± 0.63	-0.61 ± 0.69
04	2.26 ± 0.64	0.79 ± 0.47	1.74 ± 0.75	-0.77 ± 0.69
05	2.50 ± 0.66	1.09 ± 0.65	1.82 ± 0.80	-0.61 ± 0.89
06	2.71 ± 0.96	1.26 ± 0.85	1.89 ± 1.04	-0.51 ± 1.02
07	3.02 ± 1.11	1.33 ± 0.95	2.14 ± 1.35	-0.67 ± 0.91
08	3.09 ± 1.22	1.20 ± 0.96	2.18 ± 1.50	-0.47 ± 1.22
09	3.02 ± 1.11	1.33 ± 0.95	2.14 ± 1.35	-0.67 ± 0.91
10	3.30 ± 1.12	1.21 ± 1.24	1.81 ± 1.72	-0.64 ± 1.57
11	3.24 ± 1.14	1.33 ± 1.33	1.60 ± 1.68	-0.68 ± 1.57
12	3.71 ± 1.55	1.50 ± 1.46	2.08 ± 2.05	-0.81 ± 1.61
13	3.37 ± 1.23	1.67 ± 1.41	1.62 ± 1.58	-0.92 ± 1.46
14	2.92 ± 1.11	1.55 ± 1.26	1.42 ± 1.25	-0.97 ± 1.12
15	2.19 ± 1.00	1.12 ± 1.00	1.27 ± 0.87	-0.70 ± 0.83
16	1.80 ± 0.70	0.10 ± 0.61	0.87 ± 0.86	-1.01 ± 0.90
17	1.52 ± 0.69	-0.19 ± 0.61	0.72 ± 0.71	-0.86 ± 0.79
18	1.11 ± 0.57	-0.23 ± 0.58	0.21 ± 0.65	-0.50 ± 0.66
19	0.39 ± 0.25	-0.04 ± 0.32	0.10 ± 0.21	-0.03 ± 0.23

Table 1.12: CTI: Mean and standard deviation of target motion in all phases of the heart beat, relative to the reference phase. The values are taken from the contrast CTs of Pig 2.

motion phase	ABS [mm]	SI [mm]	AP [mm]	LR [mm]
01	0.29 ± 0.13	-0.00 ± 0.13	0.19 ± 0.11	0.16 ± 0.11
02	1.89 ± 0.49	0.25 ± 0.87	1.55 ± 0.56	0.25 ± 0.48
03	2.21 ± 0.55	0.48 ± 0.85	1.79 ± 0.46	0.51 ± 0.72
04	2.17 ± 0.43	0.84 ± 0.65	1.56 ± 0.39	-0.49 ± 0.98
05	4.12 ± 1.29	2.00 ± 1.31	3.40 ± 0.82	0.01 ± 0.85
06	4.43 ± 0.60	0.07 ± 1.42	4.10 ± 0.55	0.66 ± 0.68
07	4.92 ± 0.57	-0.75 ± 1.49	4.26 ± 0.54	1.47 ± 1.06
08	6.34 ± 0.54	1.26 ± 1.32	5.09 ± 0.60	3.04 ± 1.25
09	4.92 ± 0.57	-0.75 ± 1.49	4.26 ± 0.54	1.47 ± 1.06
10	4.33 ± 1.08	1.28 ± 1.14	3.50 ± 0.80	1.46 ± 1.38
11	4.41 ± 1.19	1.72 ± 1.11	3.45 ± 0.72	1.41 ± 1.51
12	4.89 ± 0.95	2.34 ± 0.86	3.68 ± 0.48	0.76 ± 2.06
13	5.53 ± 0.80	3.12 ± 0.96	4.11 ± 0.34	0.23 ± 1.87
14	4.70 ± 1.00	3.17 ± 0.96	3.03 ± 0.57	0.26 ± 1.60
15	4.31 ± 0.67	3.22 ± 0.81	2.45 ± 0.73	-0.19 ± 1.20
16	2.03 ± 0.77	0.89 ± 0.94	0.65 ± 0.62	-1.00 ± 1.12
17	2.35 ± 0.99	-0.70 ± 0.64	-0.63 ± 0.27	-2.01 ± 1.04
18	2.09 ± 0.78	-0.41 ± 0.60	-0.88 ± 0.25	-1.67 ± 0.92
19	0.71 ± 0.23	0.28 ± 0.18	-0.48 ± 0.18	-0.39 ± 0.19

Table 1.13: AV node: Mean and standard deviation of target motion in all phases of the heart beat, relative to the reference phase. The values are taken from the contrast CTs of Pig 2.

motion phase	ABS [mm]	SI [mm]	AP [mm]	LR [mm]
01	0.53 ± 0.10	0.34 ± 0.09	0.40 ± 0.07	-0.04 ± 0.05
02	1.83 ± 0.49	0.08 ± 0.10	1.73 ± 0.42	0.46 ± 0.46
03	2.10 ± 0.08	0.68 ± 0.25	1.97 ± 0.14	0.06 ± 0.09
04	3.32 ± 0.17	1.62 ± 0.37	2.86 ± 0.09	-0.11 ± 0.30
05	3.95 ± 0.29	1.35 ± 0.20	3.68 ± 0.33	0.12 ± 0.37
06	3.94 ± 0.28	1.56 ± 0.30	3.56 ± 0.20	-0.56 ± 0.20
07	4.89 ± 0.36	2.48 ± 0.23	4.20 ± 0.41	-0.09 ± 0.24
08	5.44 ± 0.25	2.68 ± 0.37	4.71 ± 0.33	0.14 ± 0.27
09	4.89 ± 0.36	2.48 ± 0.23	4.20 ± 0.41	-0.09 ± 0.24
10	5.83 ± 0.25	2.79 ± 0.41	5.08 ± 0.11	-0.21 ± 0.49
11	6.04 ± 0.19	3.71 ± 0.36	4.71 ± 0.17	-0.38 ± 0.51
12	5.86 ± 0.23	3.27 ± 0.28	4.85 ± 0.11	0.12 ± 0.22
13	5.47 ± 0.46	3.55 ± 0.56	4.13 ± 0.21	0.07 ± 0.21
14	5.25 ± 0.53	3.01 ± 0.51	4.25 ± 0.35	0.23 ± 0.50
15	4.15 ± 0.48	1.99 ± 0.28	3.52 ± 0.34	0.56 ± 0.76
16	2.98 ± 0.43	1.82 ± 0.40	2.30 ± 0.26	0.30 ± 0.36
17	2.52 ± 0.53	1.84 ± 0.45	1.45 ± 0.23	0.89 ± 0.28
18	1.05 ± 0.61	0.70 ± 0.46	0.21 ± 0.24	0.73 ± 0.38
19	0.21 ± 0.06	-0.10 ± 0.06	-0.03 ± 0.08	-0.14 ± 0.09

Table 1.14: PV: Mean and standard deviation of target motion in all phases of the heart beat, relative to the reference phase. The values are taken from the contrast CTs of Pig 3.

motion phase	ABS [mm]	SI [mm]	AP [mm]	LR [mm]
01	0.59 ± 0.27	0.05 ± 0.22	-0.07 ± 0.42	0.25 ± 0.35
02	1.39 ± 0.85	-0.21 ± 0.41	1.13 ± 0.85	0.46 ± 0.50
03	2.09 ± 0.80	-0.15 ± 0.48	1.67 ± 0.70	0.69 ± 1.01
04	2.17 ± 0.85	-0.27 ± 0.50	1.64 ± 0.73	0.81 ± 1.11
05	2.21 ± 0.89	-0.41 ± 0.57	1.94 ± 0.81	0.41 ± 0.79
06	2.39 ± 0.89	-0.48 ± 0.58	2.10 ± 0.80	0.42 ± 0.85
07	2.36 ± 0.91	-0.48 ± 0.65	2.00 ± 0.83	0.44 ± 0.92
08	2.23 ± 0.97	-0.55 ± 0.67	1.77 ± 0.89	0.47 ± 1.01
09	2.36 ± 0.91	-0.48 ± 0.65	2.00 ± 0.83	0.44 ± 0.92
10	1.79 ± 0.74	-0.19 ± 0.54	1.29 ± 0.77	0.32 ± 1.03
11	1.61 ± 0.76	0.06 ± 0.56	0.92 ± 0.85	0.16 ± 1.12
12	1.54 ± 0.57	-0.13 ± 0.43	0.53 ± 1.03	-0.17 ± 1.07
13	1.21 ± 0.52	0.01 ± 0.41	0.31 ± 0.82	-0.44 ± 0.77
14	1.53 ± 0.59	0.09 ± 0.45	-0.52 ± 1.31	-0.42 ± 0.58
15	1.38 ± 0.59	-0.13 ± 0.49	-0.52 ± 1.09	-0.59 ± 0.46
16	1.58 ± 0.77	-0.16 ± 0.59	-0.80 ± 1.21	-0.56 ± 0.53
17	1.76 ± 1.05	-0.13 ± 0.76	-1.08 ± 1.35	-0.54 ± 0.60
18	1.65 ± 0.98	-0.11 ± 0.81	-1.12 ± 1.15	-0.25 ± 0.59
19	0.63 ± 0.43	0.03 ± 0.36	-0.22 ± 0.33	-0.29 ± 0.47

Table 1.15: CTI: Mean and standard deviation of target motion in all phases of the heart beat, relative to the reference phase. The values are taken from the contrast CTs of Pig 3.

motion phase	ABS [mm]	SI [mm]	AP [mm]	LR [mm]
01	0.40 ± 0.16	0.26 ± 0.21	-0.08 ± 0.18	0.10 ± 0.15
02	1.30 ± 0.59	-0.85 ± 0.50	0.84 ± 0.43	0.20 ± 0.38
03	1.59 ± 0.38	-0.56 ± 0.45	1.37 ± 0.32	0.05 ± 0.40
04	1.63 ± 0.43	-0.16 ± 0.60	1.41 ± 0.52	0.02 ± 0.45
05	1.84 ± 0.70	0.37 ± 0.82	1.53 ± 0.74	0.19 ± 0.36
06	1.58 ± 0.67	0.08 ± 0.64	1.26 ± 0.82	0.02 ± 0.53
07	1.73 ± 0.78	-0.02 ± 0.46	1.54 ± 0.91	0.28 ± 0.36
08	1.66 ± 0.63	0.19 ± 0.47	1.08 ± 1.22	0.39 ± 0.31
09	1.73 ± 0.78	-0.02 ± 0.46	1.54 ± 0.91	0.28 ± 0.36
10	1.92 ± 0.58	0.36 ± 0.38	1.44 ± 1.17	0.04 ± 0.56
11	2.23 ± 0.63	0.89 ± 0.46	1.30 ± 0.79	1.16 ± 0.83
12	2.08 ± 0.58	0.09 ± 0.55	1.45 ± 0.42	1.03 ± 0.99
13	1.44 ± 0.55	0.90 ± 0.51	0.48 ± 0.35	0.60 ± 0.76
14	1.83 ± 0.69	1.50 ± 0.73	-0.06 ± 0.49	0.16 ± 0.86
15	1.43 ± 0.49	1.06 ± 0.49	-0.00 ± 0.46	0.17 ± 0.83
16	1.60 ± 0.29	1.25 ± 0.41	-0.48 ± 0.48	-0.10 ± 0.67
17	1.97 ± 0.40	1.48 ± 0.43	-0.68 ± 0.46	-0.88 ± 0.45
18	1.10 ± 0.48	0.77 ± 0.41	-0.44 ± 0.19	-0.44 ± 0.51
19	0.42 ± 0.14	0.08 ± 0.18	-0.22 ± 0.14	-0.12 ± 0.27

Table 1.16: AV node: Mean and standard deviation of target motion in all phases of the heart beat, relative to the reference phase. The values are taken from the contrast CTs of Pig 3.

motion phase	ABS [mm]	SI [mm]	AP [mm]	LR [mm]
01	0.97 ± 0.23	0.25 ± 0.24	-0.58 ± 0.14	-0.66 ± 0.30
02	3.86 ± 0.24	-0.46 ± 0.45	3.19 ± 0.54	-1.72 ± 1.06
03	3.38 ± 0.23	-0.62 ± 0.41	3.06 ± 0.18	-1.15 ± 0.48
04	2.87 ± 0.48	0.15 ± 0.20	1.97 ± 0.33	-2.06 ± 0.43
05	4.35 ± 0.10	-0.30 ± 0.41	3.88 ± 0.23	-1.85 ± 0.42
06	4.15 ± 0.14	0.08 ± 0.40	3.60 ± 0.26	-1.94 ± 0.54
07	3.84 ± 0.16	0.02 ± 0.31	3.40 ± 0.29	-1.68 ± 0.41
08	3.17 ± 0.17	0.04 ± 0.24	2.71 ± 0.24	-1.51 ± 0.55
09	3.84 ± 0.16	0.02 ± 0.31	3.40 ± 0.29	-1.68 ± 0.41
10	3.16 ± 0.13	0.28 ± 0.13	2.85 ± 0.20	-1.18 ± 0.59
11	3.40 ± 0.26	1.46 ± 0.54	2.18 ± 0.52	-1.91 ± 0.76
12	2.47 ± 0.37	0.04 ± 0.20	2.26 ± 0.20	-0.79 ± 0.68
13	1.56 ± 0.43	0.24 ± 0.39	1.24 ± 0.23	-0.70 ± 0.57
14	2.07 ± 0.44	0.06 ± 0.23	1.80 ± 0.30	-0.68 ± 0.78
15	2.30 ± 0.65	0.04 ± 0.26	0.60 ± 0.17	-2.20 ± 0.66
16	2.49 ± 0.63	-0.07 ± 0.17	0.19 ± 0.18	-2.47 ± 0.64
17	2.89 ± 0.74	-0.10 ± 0.13	0.41 ± 0.17	-2.84 ± 0.76
18	1.26 ± 0.26	-0.22 ± 0.11	0.73 ± 0.17	0.72 ± 0.72
19	0.85 ± 0.12	-0.18 ± 0.28	0.67 ± 0.14	0.34 ± 0.21

Table 1.17: PV: Mean and standard deviation of target motion in all phases of the heart beat, relative to the reference phase. The values are taken from the contrast CTs of Pig 4.

motion phase	ABS [mm]	SI [mm]	AP [mm]	LR [mm]
01	0.52 ± 0.31	0.22 ± 0.31	0.29 ± 0.27	-0.07 ± 0.22
02	1.72 ± 0.39	0.09 ± 0.27	1.56 ± 0.32	-0.44 ± 0.53
03	2.21 ± 0.28	0.07 ± 0.29	1.96 ± 0.22	-0.73 ± 0.66
04	2.39 ± 0.23	0.22 ± 0.32	2.14 ± 0.33	-0.63 ± 0.75
05	2.48 ± 0.38	0.14 ± 0.34	2.24 ± 0.53	-0.37 ± 0.86
06	2.48 ± 0.56	0.14 ± 0.33	2.24 ± 0.71	-0.23 ± 0.86
07	2.38 ± 0.68	0.29 ± 0.33	2.12 ± 0.86	-0.25 ± 0.80
08	2.34 ± 0.80	0.41 ± 0.38	1.99 ± 1.00	-0.30 ± 0.86
09	2.38 ± 0.68	0.29 ± 0.33	2.12 ± 0.86	-0.25 ± 0.80
10	3.05 ± 1.06	0.70 ± 0.59	2.45 ± 1.36	-0.59 ± 1.19
11	3.13 ± 1.03	0.81 ± 0.67	2.64 ± 1.17	-0.49 ± 1.09
12	2.82 ± 0.80	0.80 ± 0.63	2.44 ± 0.84	-0.37 ± 0.87
13	2.38 ± 0.74	0.56 ± 0.62	2.19 ± 0.68	-0.08 ± 0.51
14	2.17 ± 0.63	0.45 ± 0.52	2.02 ± 0.58	0.13 ± 0.48
15	2.05 ± 0.45	0.22 ± 0.37	1.92 ± 0.46	0.30 ± 0.47
16	1.98 ± 0.41	-0.10 ± 0.43	1.79 ± 0.37	0.32 ± 0.68
17	1.68 ± 0.51	-0.03 ± 0.56	1.42 ± 0.41	0.41 ± 0.64
18	1.12 ± 0.43	-0.02 ± 0.32	0.87 ± 0.39	0.37 ± 0.54
19	0.48 ± 0.22	-0.11 ± 0.19	0.29 ± 0.29	0.09 ± 0.22

Table 1.18: CTI: Mean and standard deviation of target motion in all phases of the heart beat, relative to the reference phase. The values are taken from the contrast CTs of Pig 4.

motion phase	ABS [mm]	SI [mm]	AP [mm]	LR [mm]
01	0.24 ± 0.07	0.11 ± 0.16	0.01 ± 0.11	0.07 ± 0.07
02	0.73 ± 0.16	0.55 ± 0.20	0.26 ± 0.29	-0.10 ± 0.24
03	1.47 ± 0.47	0.41 ± 0.41	1.19 ± 0.36	-0.59 ± 0.39
04	1.66 ± 0.47	0.50 ± 0.34	1.46 ± 0.37	-0.09 ± 0.59
05	2.18 ± 0.34	0.44 ± 0.26	2.04 ± 0.31	0.20 ± 0.54
06	2.64 ± 0.36	0.09 ± 0.13	2.55 ± 0.40	0.53 ± 0.39
07	2.63 ± 0.43	0.07 ± 0.26	2.54 ± 0.41	0.51 ± 0.43
08	2.70 ± 0.61	0.46 ± 0.48	2.56 ± 0.56	0.26 ± 0.52
09	2.63 ± 0.43	0.07 ± 0.26	2.54 ± 0.41	0.51 ± 0.43
10	3.52 ± 0.53	1.76 ± 0.65	2.86 ± 0.58	0.12 ± 0.75
11	3.52 ± 0.49	2.02 ± 0.56	2.71 ± 0.56	0.10 ± 0.74
12	3.67 ± 0.63	1.97 ± 0.51	2.96 ± 0.59	0.47 ± 0.64
13	3.95 ± 0.83	2.27 ± 0.59	3.12 ± 0.77	0.36 ± 0.57
14	3.11 ± 0.69	1.72 ± 0.66	2.44 ± 0.75	-0.17 ± 0.43
15	1.98 ± 0.40	0.98 ± 0.37	1.56 ± 0.51	-0.16 ± 0.53
16	1.42 ± 0.32	0.70 ± 0.29	1.05 ± 0.49	-0.34 ± 0.29
17	1.19 ± 0.32	0.55 ± 0.28	0.55 ± 0.38	-0.69 ± 0.46
18	0.94 ± 0.23	0.66 ± 0.25	0.02 ± 0.24	-0.54 ± 0.30
19	0.46 ± 0.20	0.12 ± 0.07	0.12 ± 0.20	-0.29 ± 0.31

Table 1.19: AV node: Mean and standard deviation of target motion in all phases of the heart beat, relative to the reference phase. The values are taken from the contrast CTs of Pig 4.

motion phase	ABS [mm]	SI [mm]	AP [mm]	LR [mm]
01	0.27 ± 0.08	0.17 ± 0.05	-0.17 ± 0.12	0.01 ± 0.07
02	0.52 ± 0.18	0.11 ± 0.04	0.16 ± 0.25	-0.36 ± 0.27
03	2.19 ± 0.21	0.13 ± 0.17	1.99 ± 0.18	-0.82 ± 0.38
04	2.30 ± 0.23	0.17 ± 0.12	2.16 ± 0.22	-0.71 ± 0.27
05	2.30 ± 0.23	0.17 ± 0.08	2.22 ± 0.24	-0.52 ± 0.22
06	2.52 ± 0.32	0.24 ± 0.17	2.44 ± 0.32	-0.40 ± 0.36
07	2.42 ± 0.37	0.28 ± 0.10	2.32 ± 0.39	-0.50 ± 0.36
08	3.05 ± 0.33	0.42 ± 0.13	2.84 ± 0.40	-0.86 ± 0.52
09	2.42 ± 0.37	0.28 ± 0.10	2.32 ± 0.39	-0.50 ± 0.36
10	3.63 ± 0.67	0.77 ± 0.22	3.18 ± 0.44	-1.43 ± 0.81
11	3.49 ± 0.55	0.98 ± 0.20	3.16 ± 0.47	-0.95 ± 0.62
12	2.92 ± 0.60	1.03 ± 0.30	2.59 ± 0.47	-0.66 ± 0.59
13	2.39 ± 0.55	0.75 ± 0.31	2.16 ± 0.42	-0.56 ± 0.48
14	1.96 ± 0.40	0.65 ± 0.18	1.72 ± 0.34	-0.54 ± 0.41
15	2.04 ± 0.46	0.40 ± 0.21	1.67 ± 0.28	-1.04 ± 0.48
16	2.01 ± 0.39	0.69 ± 0.27	1.37 ± 0.25	-1.24 ± 0.40
17	1.31 ± 0.38	0.64 ± 0.24	0.62 ± 0.20	-0.89 ± 0.41
18	0.74 ± 0.40	0.55 ± 0.31	0.09 ± 0.27	-0.36 ± 0.31
19	0.41 ± 0.15	0.13 ± 0.09	-0.06 ± 0.19	-0.26 ± 0.25

Table 1.20: AV node: Mean and standard deviation of target motion in all phases of the heart beat, relative to the reference phase. The values are taken from the native CTs of Pig 3.

motion phase	ABS [mm]	SI [mm]	AP [mm]	LR [mm]
01	0.07 ± 0.02	0.01 ± 0.03	-0.03 ± 0.03	-0.02 ± 0.03
02	0.12 ± 0.06	0.09 ± 0.06	0.04 ± 0.04	-0.04 ± 0.03
03	0.09 ± 0.05	-0.02 ± 0.03	0.05 ± 0.05	-0.01 ± 0.06
04	0.19 ± 0.07	0.13 ± 0.07	0.09 ± 0.08	0.03 ± 0.05
05	0.16 ± 0.07	0.05 ± 0.07	0.11 ± 0.08	-0.00 ± 0.06
06	0.18 ± 0.08	0.12 ± 0.10	0.06 ± 0.08	-0.01 ± 0.05
07	0.19 ± 0.08	0.16 ± 0.09	0.03 ± 0.05	-0.04 ± 0.05
08	0.13 ± 0.05	0.06 ± 0.08	-0.01 ± 0.05	-0.06 ± 0.06
09	0.19 ± 0.08	0.16 ± 0.09	0.03 ± 0.05	-0.04 ± 0.05
10	0.17 ± 0.05	0.10 ± 0.05	-0.10 ± 0.08	-0.03 ± 0.07
11	0.16 ± 0.07	0.05 ± 0.03	-0.12 ± 0.08	0.05 ± 0.05
12	0.23 ± 0.08	0.11 ± 0.03	-0.14 ± 0.09	0.11 ± 0.06
13	0.13 ± 0.04	-0.00 ± 0.05	-0.06 ± 0.08	0.06 ± 0.05
14	0.10 ± 0.04	-0.05 ± 0.02	0.01 ± 0.07	0.03 ± 0.06
15	0.11 ± 0.05	0.01 ± 0.04	0.01 ± 0.07	-0.01 ± 0.09
16	0.12 ± 0.06	0.03 ± 0.03	0.04 ± 0.07	-0.02 ± 0.10
17	0.08 ± 0.04	-0.01 ± 0.03	0.01 ± 0.07	-0.01 ± 0.04
18	0.10 ± 0.04	-0.06 ± 0.03	-0.00 ± 0.06	-0.03 ± 0.03
19	0.05 ± 0.02	0.01 ± 0.03	-0.02 ± 0.04	-0.00 ± 0.03

Table 1.21: Pig 1, AV node

Case	motion period	motion starting phase	Margin	rescan no.	D5-D95 [%]	V95 [%]	V107 [%]
STATIC	-	-	5mm	-	5.66	100.00	0.00
INTERPLAY	0.7s	0	5mm	-	13.94	100.00	51.85
INTERPLAY	0.7s	90	5mm	-	13.64	90.74	6.67
INTERPLAY	0.5s	0	5mm	-	16.37	73.33	4.81
INTERPLAY	0.5s	90	5mm	-	8.19	100.00	32.96
RESCANNING	0.7s	0	5mm	10	6.26	100.00	0.00
RESCANNING	0.7s	90	5mm	10	4.70	100.00	0.00
RESCANNING	0.5s	0	5mm	10	5.79	100.00	0.00
RESCANNING	0.5s	90	5mm	10	4.24	100.00	0.00
RESCANNING	0.7s	0	5mm	15	4.88	100.00	0.00
RESCANNING	0.7s	90	5mm	15	3.91	100.00	0.00
RESCANNING	0.5s	0	5mm	15	5.37	100.00	0.00
RESCANNING	0.5s	90	5mm	15	5.80	100.00	0.00

Table 1.22: Pig 2, AV node

Case	motion period	motion starting phase	Margin	rescan no.	D5-D95 [%]	V95 [%]	V107 [%]
STATIC	-	-	5mm	-	4.41	100.00	0.00
INTERPLAY	0.7s	0	5mm	-	7.20	97.55	0.00
INTERPLAY	0.7s	90	5mm	-	6.19	99.02	0.00
INTERPLAY	0.5s	0	5mm	-	9.33	91.18	0.00
INTERPLAY	0.5s	90	5mm	-	10.90	99.51	4.90
RESCANNING	0.7s	0	5mm	10	3.66	100.00	0.00
RESCANNING	0.7s	90	5mm	10	7.90	98.53	0.00
RESCANNING	0.5s	0	5mm	10	6.20	100.00	9.31
RESCANNING	0.5s	90	5mm	10	4.03	100.00	0.00
RESCANNING	0.7s	0	5mm	15	4.35	100.00	0.00
RESCANNING	0.7s	90	5mm	15	6.98	100.00	0.00
RESCANNING	0.5s	0	5mm	15	7.27	99.51	0.00
RESCANNING	0.5s	90	5mm	15	3.61	100.00	0.00

Table 1.23: Pig 3, AV node

Case	motion period	motion starting phase	Margin	rescan no.	D5-D95 [%]	V95 [%]	V107 [%]
STATIC	-	-	5mm	-	2.20	100.00	0.00
INTERPLAY	0.7s	0	5mm	-	5.64	55.88	0.00
INTERPLAY	0.7s	90	5mm	-	6.98	100.00	0.00
INTERPLAY	0.5s	0	5mm	-	8.83	92.94	0.00
INTERPLAY	0.5s	90	5mm	-	5.22	100.00	0.00
RESCANNING	0.7s	0	5mm	10	4.89	100.00	0.00
RESCANNING	0.7s	90	5mm	10	6.22	100.00	0.00
RESCANNING	0.5s	0	5mm	10	4.42	100.00	0.00
RESCANNING	0.5s	90	5mm	10	3.42	100.00	0.00
RESCANNING	0.7s	0	5mm	15	5.85	99.41	0.00
RESCANNING	0.7s	90	5mm	15	5.57	100.00	0.00
RESCANNING	0.5s	0	5mm	15	4.70	100.00	0.00
RESCANNING	0.5s	90	5mm	15	5.38	100.00	0.00

Table 1.24: Pig 4, AV node

Case	motion period	motion starting phase	Margin	rescan no.	D5-D95 [%]	V95 [%]	V107 [%]
STATIC	-	-	5mm	-	5.53	100.00	0.00
INTERPLAY	0.7s	0	5mm	-	13.82	83.67	0.00
INTERPLAY	0.7s	90	5mm	-	12.81	74.29	0.41
INTERPLAY	0.5s	0	5mm	-	17.58	80.61	17.14
INTERPLAY	0.5s	90	5mm	-	21.75	44.49	0.00
RESCANNING	0.7s	0	5mm	10	5.25	100.00	0.00
RESCANNING	0.7s	90	5mm	10	5.95	97.76	0.00
RESCANNING	0.5s	0	5mm	10	5.09	100.00	0.20
RESCANNING	0.5s	90	5mm	10	5.44	98.37	0.00
RESCANNING	0.7s	0	5mm	15	4.99	100.00	0.00
RESCANNING	0.7s	90	5mm	15	5.55	100.00	0.00
RESCANNING	0.5s	0	5mm	15	2.96	100.00	0.00
RESCANNING	0.5s	90	5mm	15	4.69	100.00	0.00

Bibliography

[afib] Atrial fibrillation Resources for patients, a-fib.com

[Bla13] Blanck O, Bode F, Gebhard M, Hunold P, Brandt S, Bruder R, Schweikard A, Grossherr M, Rades D and Dunst J: Radiochirurgisch erzeugte Läsionen im Antrum der Pulmonarvenen: Vorläufige Ergebnisse im Tiermodell und mögliche Implikationen für die Behandlung von Vorhofflimmern; DEGRO 2013

[Bro07] Brock et al: Image Registration in IMRT, IGRT and SBRT; in C.Meyer (ed): IMRT-IGRT-SBRT; Front Radiat Ther Oncol; Karger; 2007

[Gra12] Graeff C, Durante M and Bert C: Motion mitigation in intensity modulated particle therapy by internal target volumes covering range changes; Med. Phys. 39 (10); 2012

[Ric13] Richter D, Schwarzkopf A, Trautmann J, Krämer M, Durante M, Jäkel O, Bert C: Upgrade and benchmarking of a 4D treatment planning system for scanned ion beam therapy; Med Phys.; 40(5); 2013

[Sha10] Sharma A, Wong D, Weidlich G, Fogarty T, Jack A, Sumanaweera T, Maguire P: Noninvasive stereotactic radiosurgery (CyberHeart) for creation of ablation lesions in the atrium; Heart Rhythm 7(6); 802-810; 2010 NCBINCBI Logo NCBINCBI Logo

[Sharp07] Sharp CG, Kandasamy N, Singh H and Folkert M: GPU-based streaming architectures for fast cone-beam CT image reconstruction and demons deformable registration; Phys. Med. Biol.; 52(19); 5771-5783; 2007

[Shack10] Shakleford JA, Kandasamy N and Sharp GC: On developing B-spline registration algorithms for multi-core processors; Physics in Medicine and Biology; 55(21); 2010

[Zen10] Zenklusen SM, Pedroni E and Meer D: A study on repainting strategies for treating moderately moving targets with proton pencil beam scanning at the new gantry 2 at PSI; Physics in Medicine and Biology; 55(17); 5103-5121; 2010

[Cri98] Crick SJ, Sheppard MN, Ho SY, Gebstein L, Anderson RH: Anatomy of the pig heart: comparisons with normal human cardiac structure; J Anat.; 193(Pt 1): 105?119; 1998

[Hug86] Hughes HC: Swine in cardiovascular research; Laboratory Animal Science 36, 348-350; 1986

[Lum66] Lumb GD: Experimentally induced cardiac failure in swine: pathological changes; Swine in Biomedical Research (ed. Bustad LK, McClellan RO), pp. 389-403. Pacific Northwest Laboratory, Seattle, Washington: Batelle Memorial Institute; 1966

[Dou72] Douglas WR: Of pigs and men and research: a review of applications and analogies of the pig, Sus scrofa, in human medical research: Space Life Sciences 3, 226-234; 1972

[Coo91] Cooper DKC, Ye Y, Rolf LL, Zuhdi N: The pig as potential organ donor for man. In Xenotransplantation: The Transplantation of Organs and Tissues Between Species (ed. Cooper DKC, Kemp E, Reemtsma K, White DJG), pp. 480-500. Berlin: Springer; 1991

[Whi93] White D, Wallwork J: Xenografting: probability, possibility, or pipe-dream?; Lancet 342; 879-880; 1993

[Son14] Song L, Lehmann HI, Cusma JT, Christner JA, Misiri J, Johnson SB, Parker KD, Takami M, Miller RC, Herman MG and Packer DL: Intensity Modulated Proton Therapy using Pencil Beam Scanning as a Catheter-free Ablation Approach: A 4D Treatment Planning Study in the Porcine Model; HRS Abstract; 2014